Active Fault Systems in the Inner Northwest Apennines, Italy: A Reappraisal One Century after the 1920 Mw 6.5 Fivizzano Earthquake

Giancarlo Molli, Isabelle Manighetti, Rick Bennett, Jacques Malavieille, Enrico Serpelloni, Fabrizio Storti, Tiziano Giampietro, Aurelien Bigot, Gabriele Pinelli, Serena Giacomelli, et al.

geosciences

MDPI

Review

Active Fault Systems in the Inner Northwest Apennines, Italy: A Reappraisal One Century after the 1920 Mw ~6.5 Fivizzano Earthquake

Giancarlo Molli [1,*], Isabelle Manighetti [2], Rick Bennett [3], Jacques Malavieille [4], Enrico Serpelloni [5], Fabrizio Storti [6], Tiziano Giampietro [2], Aurelien Bigot [4], Gabriele Pinelli [1], Serena Giacomelli [7], Alessio Lucca [6], Luca Angeli [1] and Lorenzo Porta [1]

1 Dipartimento Scienze Della Terra, Università di Pisa, 56126 Pisa, Italy; g.pinelli@marmotest.com (G.P.); lucaangeli12@gmail.com (L.A.); portalorenzo4@gmail.com (L.P.)
2 Université Côte d'Azur, Observatoire de la Côte d'Azur, French Research Institute for Development (IRD), French National Center for Scientific Research (CNRS), Géoazur, Sophia Antipolis, 06905 Valbonne, France; manighetti@geoazur.unice.fr (I.M.); giampietro@geoazur.unice.fr (T.G.)
3 Department of Geosciences, University of Arizona, Tucson, AZ 85721, USA; rb0@email.arizona.edu
4 Géosciences Montpellier, Université de Montpellier, 34095 Montpellier, France; j.malavie@gmail.com (J.M.); aurelien.bigot@hotmail.fr (A.B.)
5 Istituto Nazionale di Geofisica e Vulcanologia, Osservatorio Nazionale Terremoti, 40128 Bologna, Italy; enrico.serpelloni@ingv.it
6 Natural and Experimental Tectonics Research Group, Department of Chemistry, Life Sciences and Environmental Sustainability, University of Parma, 43124 Parma, Italy; fabrizio.storti@unipr.it (F.S.); alessio.lucca@unipr.it (A.L.)
7 Dipartimento di Scienze Biologiche, Geologiche e Ambientali, Università di Bologna, 40126 Bologna, Italy; giacserena@gmail.com
* Correspondence: giancarlo.molli@unipi.it

Abstract: Based on the review of the available stratigraphic, tectonic, morphological, geodetic, and seismological data, along with new structural observations, we present a reappraisal of the potential seismogenic faults and fault systems in the inner northwest Apennines, Italy, which was the site, one century ago, of the devastating Mw ~6.5, 1920 Fivizzano earthquake. Our updated fault catalog provides the fault locations, as well as the description of their architecture, large-scale segmentation, cumulative displacements, evidence for recent to present activity, and long-term slip rates. Our work documents that a dense network of active faults, and thus potential earthquake fault sources, exists in the region. We discuss the seismogenic potential of these faults, and propose a general tectonic scenario that might account for their development.

Keywords: active faults; earthquakes; inner northwest Apennines; current deformation; satellite geodesy

Citation: Molli, G.; Manighetti, I.; Bennett, R.; Malavieille, J.; Serpelloni, E.; Storti, F.; Giampietro, T.; Bigot, A.; Pinelli, G.; Giacomelli, S.; et al. Active Fault Systems in the Inner Northwest Apennines, Italy: A Reappraisal One Century after the 1920 Mw ~6.5 Fivizzano Earthquake. *Geosciences* **2021**, *11*, 139. https://doi.org/10.3390/geosciences11030139

Academic Editors: Jesus Martinez-Frias and Rodolfo Carosi

Received: 31 January 2021
Accepted: 12 March 2021
Published: 18 March 2021

1. Introduction

Earthquake data, including instrumental and historical earthquakes, are critical information to constrain seismic-hazard assessment [1–4]. However, these data cover periods of time that are generally much shorter than the recurrence times of large earthquakes (i.e., with Mw $\geq$ 6.0) on a given fault and regionally, especially in areas of low deformation rates [5–7], as is the case in Italy. Paleoseismological data [8] may complete and complement the seismic catalogs, but paleoseismological studies are generally difficult to conduct extensively—as is the case in Italy at the present moment—and they generally recover partial information on the past earthquakes. Nevertheless, earthquakes result from the rupture of tectonic faults that are generally long-lived features, and it has been shown that documenting these long-term faults provides critical insights to anticipate some of the properties of the large earthquakes these faults may produce in the future [5,6,9]. On the

other hand, identifying where seismogenic faults are in a region is key to anticipate where earthquakes might occur in the future (e.g., [9]).

Faults have intrinsic properties, such as a 3D overall architecture, a lateral segmentation of their principal trace, a certain degree of structural maturity, a given average slip rate, etc., and these properties have been shown to control, at least partly, the earthquake behavior [10–12]. In particular, the fault structural maturity, which relates to the fault slip longevity and rate over geological time, markedly impacts the geometrical and mechanical properties of the fault, which in turn controls the earthquake rupture size (rupture length and slip amplitude) and "energy" (i.e., stress drop); the more immature a fault, the greater its capacity to produce large stress drop, and hence highly damaging earthquakes [11,13,14]. Therefore, identifying seismogenic faults in a given region and documenting their general properties (lateral segmentation, connection to other faults, cumulative displacements, slip rates, etc.) constitutes a fundamental basis to implement and improve the seismotectonic models that are used as input for seismic hazard estimates [9].

In the present study, we conduct this work in the inner northwest Apennines region of Italy. That region was the site, one century ago, of a major devastating earthquake, the 1920 Fivizzano event, the magnitude of which is estimated at Mw 6.5, similar to that of the dramatic main shock of the 2016 Central Italy earthquake sequence [15]. This region also hosted several other moderate to large historical earthquakes over the last few centuries. Despite the occurrence of all these earthquakes, the Italian database of seismogenic structures (DISS-INGV) [16] includes only two seismic sources in the whole region. We document here that many more potential earthquake fault sources exist in the region (some are referred in the Ithaca fault catalog, ISPRA [17]), and should be taken into account in seismic-hazard evaluation.

Based on a comprehensive review of the available geological, tectonic, chronological, morphological, geodetic, and seismological (instrumental and historical) data for the inner northwest Apennines, along with new tectonic data from our own work, we present a reappraisal of the active or possibly active seismogenic faults and fault systems in the internal Apennines north of the Arno river. Our updated fault catalog provides the fault locations, as well as the description of their architecture, large-scale segmentation, cumulative displacements, evidence for recent to present activity, and long-term slip rates. It also includes the offshore domains of the northern Tyrrhenian coast so far ignored in previous compilations [16,17]. Our work eventually allows us to discuss the seismogenic potential of the identified faults, while proposing a general tectonic scenario accounting for these faults.

2. Main Structural Domains in the Northern Apennines

The northern Apennines (Figure 1) are the result of the Neogene subduction of the Adria continental crust and the overlying remnants of a former intraoceanic accretionary wedge [18–20]. The latter is represented by the so-called Ligurian and sub-Ligurian units, which may be observed superimposed to the Tuscan and Romagna–Umbria continental-derived cover and basement of the distal to proximal Adria margin [18–21]. After the inception of the continental subduction during the Oligocene, parts of the Adria continental margin were imbricated and incorporated into the orogenic wedge at a shallow crustal depth (e.g., the Tuscan Nappe), whereas other portions were underplated at deeper crustal levels (e.g., the Tuscan Metamorphic units) and lately exhumed at the surface within tectonic windows in the internal, Tyrrhenian side of the orogen [19–21].

The Neogene-to-recent tectonic evolution of the Apennines has been characterized by contractional tectonic activity in the foreland, accompanied by extension in the internal domain [22–24]. This deformation has produced a great density and variety of fault systems with different kinematics, which may be seen as defining different morphostructural domains (Figure 1), as described below [25–29].

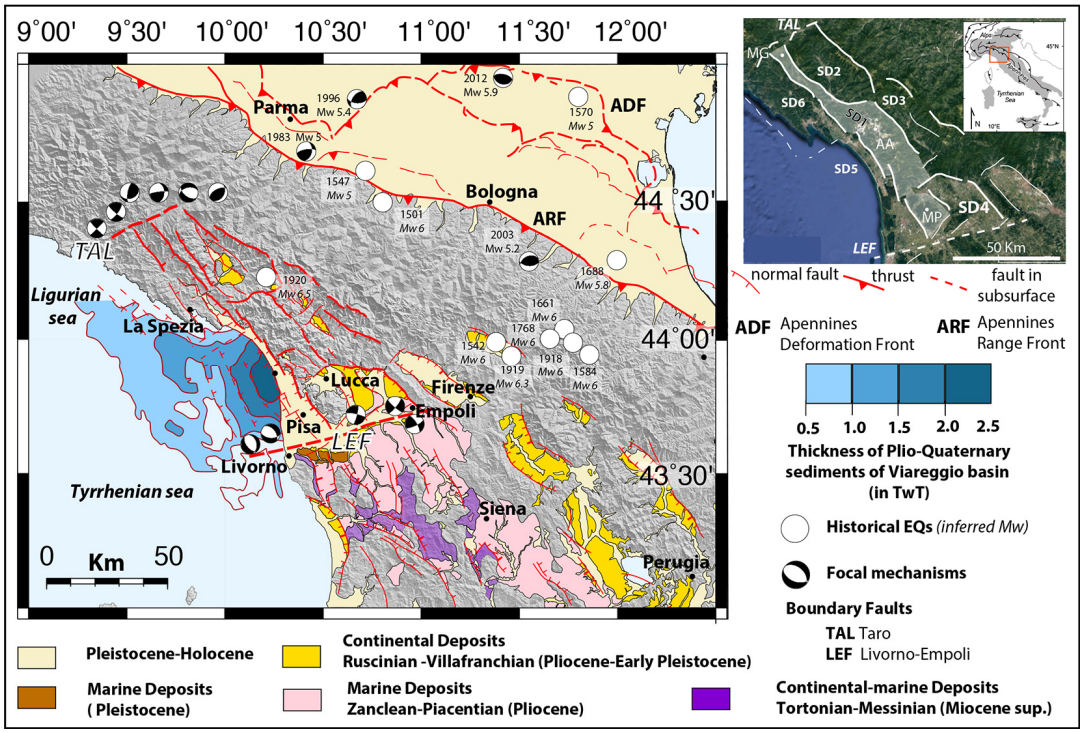

Figure 1. Simplified geological and structural map of the northern Apennines emphasizing the Neogene tectonics in the investigated area. Structural domains (SDs) discussed in the paper are shown in the Google Earth inset. AA: Alpi Apuane; LEF: Livorno–Empoli Fault; MG: Mt. Gottero; MP: Mt. Pisano; TAL: Taro Line. TAL and LEF bound the region of study. Offshore sediment thickness are after [30,31], and earthquakes and focal mechanisms are from the INGV archive [2,32].

The major fault systems in the external domain are the contractional fronts, divided into the northern Apennines Deformation Front (ADF) and the Apennines Range Front (ARF). The northeast Apennines Deformation Front is presently primarily buried beneath the Po Valley and extends offshore in the western Adriatic Sea [23,24,28,29]. Recent seismicity, including the 2012 Emilia Mw 5.9 thrust earthquake [4,33], along with geomorphic studies [29], clearly show that folding and thrusting associated with the ADF are currently active. The Apennines Range Front [25,27–29] lies some 60 km to the southwest of the ADF. The ARF front is marked by a transition from gently dipping alluvial strata in the Po basin to uplifted bedrock in the Apennines, presently standing up to 2000 m above the Po plain near the orographic divide. Different authors have provided evidence that the topography of the range front represents the forward-dipping limb of an anticline overlying a fairly steeply dipping blind reverse fault [29,34]. Similarly to the ADF, the ARF is currently active, as documented by GPS measurements of ongoing crustal deformation [25] and instrumental seismic activity including some recent moderate earthquakes, such as the 1983 Mw 5.0 "Parma" and the 2003 Mw 5.2 "Monghidoro" thrust ruptures [1,2,4,35,36]. Historical earthquakes are also reported on the ARF, such as the 1501 Mw 5 "Modenese", the 1547 Mw 6 "Reggiano", and the 1688 Mw 5.8 "Romagna" earthquakes [37].

The inner Apennines are characterized by a lower frequency of earthquakes, yet of significant magnitude, with most of them showing a normal faulting slip mode. Among the several large earthquakes that have occurred in the region, there are the 1542 and the 1919 "Mugello" events (Mw 6.0 and Mw 6.4, respectively), the 1584, 1661, 1768, and 1918 events in the "Forlivese" region (all ~ Mw 6), and the 1920 ~Mw 6.5 Fivizzano earthquake [35,37,38]. This latter earthquake will be discussed in some detail in the following.

3. Faulting in Main Morphostructural Domains

The characteristics of the faults described in this section are summarized in Table S1. The fault and geological maps described below are derived from the combination of available studies to which we refer, and from our work.

The study area extends over more than 6000 km^2 on the Tyrrhenian side of the northern Apennines (Figure 1). From a morphostructural point of view, it is limited by the main Apenninic orographic divide to the east/northeast, and by the northern Tyrrhenian–Ligurian Sea to the west/southwest. More precisely, the northern boundary of the region coincides with an alignment of reliefs with a transversal, nearly east–west trend bounding the Taro valley, whereas to the South, the region is bounded by the shallow hilly reliefs between Livorno and Empoli (Figure 1).

These northern and southern boundaries represent the surface expression of crustal/lithospheric discontinuities [39,40], corresponding to the westernmost part of the Taro Line (TAL) to the north [18,41–44] and to the westernmost part of the Livorno–Sillaro Line [45–47], called the Livorno–Empoli Fault (LEF in Figure 1), to the south. The Taro Line, already recognized in early studies (refs. in [39,41,42,48]), has been described in different contributions due to its prominent morphological signature [41–43] and seismic activity [4,35,49]. In the most recent interpretations, its westernmost segment, within our region of interest, is associated with a lateral ramp of a basement thrust, named the Taro lateral ramp, that would accommodate a NE–SW crustal shortening [42–44,50]. On the other hand, the Livorno–Empoli Fault coincides with a significant lateral change in the thickness of the crust, with the northern Tuscany crust being ~28 km thick north of the fault and ~20 km thick south of it [47,51,52]. The geology also changes across the LEF, with the base of Late Miocene marine basins exposed at the surface south of the fault (in the southern Tuscany Tectonic Province), while the same horizons are buried in the subsurface north of it (e.g., in the Viareggio basin). Both the Taro Line and the Livorno–Empoli Fault are associated with well-documented deformations within the Neogene–Quaternary deposits [44,46,47]. Their activity is still ongoing, as attested by historical and instrumentally recorded seismicity [49,51,52] (Figure 1).

In between the TAL and LEF, first-order physiographic and structural features allow the definition of six principal structural domains (SDs) (Figure 1). These are related to a set of ranges with a dominant NW to NNW trend (Apenninic trend) separated by intramontane or continental/marine morphotectonic depressions. The division into domains mainly aims to simplify their description.

The structural domain SD1 is bounded toward the Apenninic divide by the upper Lunigiana and Garfagnana grabens, which form the structural domains SD2 and SD3 to the north, and by the Lucca plain and the Montecarlo–Vinci hills (structural domain SD4) to the south. West of SD1 in the southern part of the Alpi Apuane–Mt. Pisano, the structural domain SD5 corresponds to the Versilia and Pisa plains, which are parts of a major submarine half-graben, the Viareggio basin. The latter grades northward to the structural domain SD6, a mixed on-land/offshore domain hosting the Vara Valley–lower Lunigiana tectonic depressions and the western promontory of La Spezia. Plio-Quaternary stratigraphic units form the sedimentary filling of the intramontane or continental/marine domains in all these zones (Figure 2). These Plio-Quaternary sedimentary records will be used to document the neotectonic activity of the principal faults and systems in each of the six structural domains.

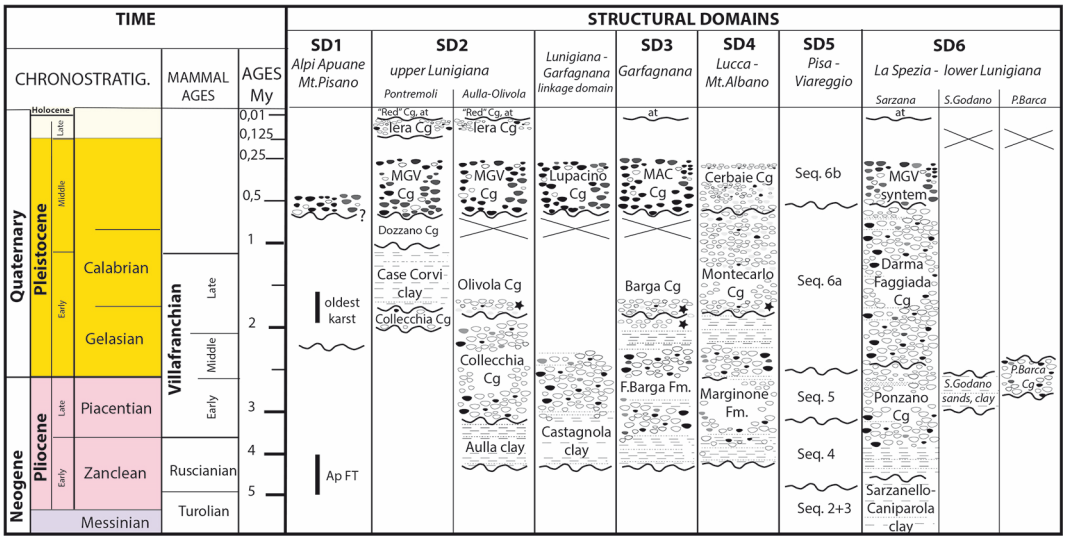

Figure 2. Schematic frame and correlations of continental–marine Plio-Quaternary sedimentary successions in the different structural domains described (MGV and MAC mean Magra Valley and Macigno-rich conglomerates, respectively).

4. Plio-Quaternary Stratigraphic Units, Fault Systems, Time of Activity and Displacements

4.1. Structural Domain SD1: The Mt. Gottero–Alpi Apuane–Mt. Pisano

The present-day large-scale geomorphology of the structural domain SD1 is dominated by the sharp relief of the Alpi Apuane (AA in inset of Figure 1), with its highest summits (~2000 m) only a few kilometers away from the Tyrrhenian coastline. North of the Alpi Apuane, the relief reaches ~1600 m on Mt. Gottero, whereas to the south Mt. Pisano stands at an elevation of ~900 m. The metamorphic units of the Alpi Apuane and the southernmost Mt. Pisano have been the object of low-temperature thermochronological investigations [53,54], which constrained the latest stages of exhumation as occurring in the last 4–5 myrs. This exhumation is taken to have resulted from erosion associated with normal faulting along the steep bounding faults (Figure 1) separating the exposure of the metamorphic rocks from the surroundings [50,54]. The estimated exhumation rates are about 0.5–0.8 mm/yr [54,55]. Within this SD1 domain, few remnants of continental deposits of Pleistocene (or Middle Pleistocene?) age (Figure 2) may be found locally, at an elevation of ~1000 m in the southeast Alpi Apuane [56,57].

4.2. Structural Domain SD2: Upper Lunigiana

Structural domain SD2 includes the upper Lunigiana, a valley hosting the upper course of the Magra River (Figure 3). Continental stratigraphic sequences are observed in the northwest part close to Pontremoli and in the central-southeast area close to Aulla (Figures 2 and 3). The deposits in these two areas show the same sedimentary evolution with a transition from fluvio-lacustrine to fluvial environments, and a diachronous sedimentation (Figure 2).

In the southernmost sector, the Aulla clays, with an estimated thickness of 70–80 m [58,59], mainly consist of fine-grained lithofacies, with medium to thick coarse-grained interbeds of sandstones and conglomerates. The overlaying coarse-grained Collecchia conglomerates, interpreted as alluvial fan deposits formed in a braided fluvial environment, directly cover the bedrock in the marginal zone of the former basin and overlay the Aulla clays in the depocentral area, where they show a thickness of ~150 m [58,59].

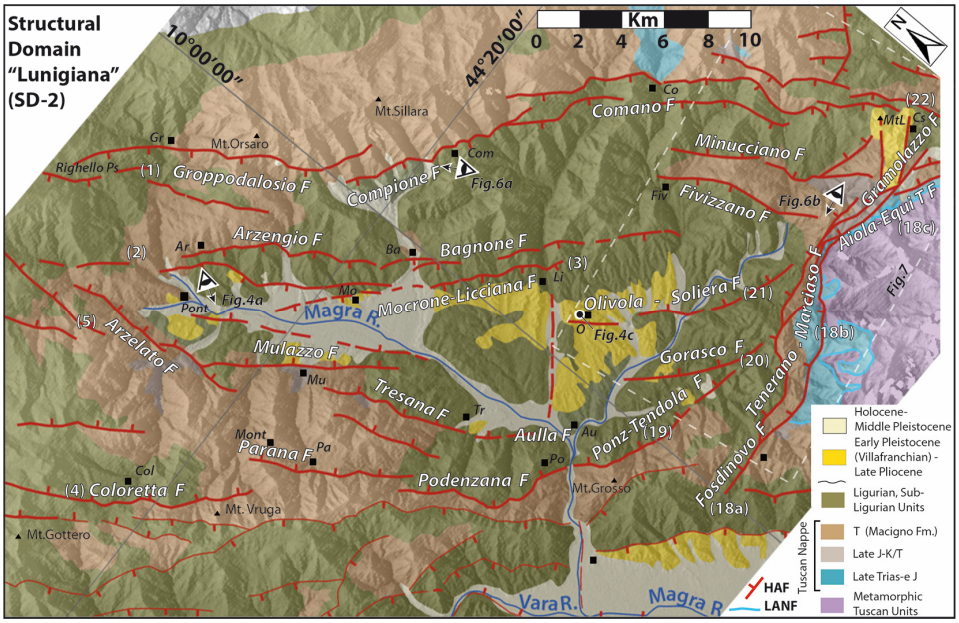

Figure 3. Main fault systems and geology in structural domain SD2 (Lunigiana). The map is derived from [57–60] and our work. Fault identification numbers are as reported in Table S1. HAF: steep normal faults (thicker lines for those described); LANF: low-angle detachment faults; Ar: Arzengio; Au: Aulla; Ba: Bagnone; Co: Comano; Col: Coloretta; Com: Compione; Cs: Castagnola; Fiv. Fivizzano; Gr: Groppodalosio; Li: Licciana; Mont: Montereggio; MtL: Mt. Lupacino; O: Olivola; Pa: Parana; Po: Podenzana; Pont: Pontremoli.

The Olivola conglomerates unconformably overlay the Collecchia conglomerates and are only preserved close to the Olivola village. The sequence starts with clay–sandy deposits, containing the Olivola mammals remains of Late Villafranchian age [59–62], followed by clast-supported and well-cemented conglomerates and sandstones (Figures 2–4). The conglomerates, with a thickness of about 60 m in the type-area, include clasts of metamorphic rocks belonging to the Tuscan metamorphic units.

The sequence exposed close to Pontremoli starts with a ~10 m thick polygenic conglomerate followed by the Case Corvi clays, which mainly consist of blue-grey clays and silty clays with lignite fragments, grading to sandstones and conglomerates, which become more abundant and coarser-grained in the upper portion. The land fossil remains and pollen in the finer-grain deposits allow attributing the unit to the Late Villafranchian [63–65].

The following Dozzano conglomerates mainly consist of coarse-grained sediments and subordinate lenses of sandstones and clays. The sequence, etheropic with the Case Corvi clays, is characterized by channel-shape deposits of well-sorted polygenic conglomerate with poor matrix and with thin sandstone and clay levels. It is followed by a polygenic conglomerate with clay matrix and a thickness of ~20 m. The sedimentary facies suggest debris-flow processes that prograded from the margins basinward. The unit is suggestive of Early Pleistocene, since its deposition occurred between that of the Case Corvi clays and that of the Magra Valley Conglomerates [58,66].

The two continental Villafranchian sequences of the Aulla–Olivola and Pontremoli areas have been related by some authors to independent and distinct basins [59,65–67], whereas other authors have interpreted them as being connected to a single "Lunigiana basin" with a diachronous development and a later segmentation during the post-Villafranchian time [58].

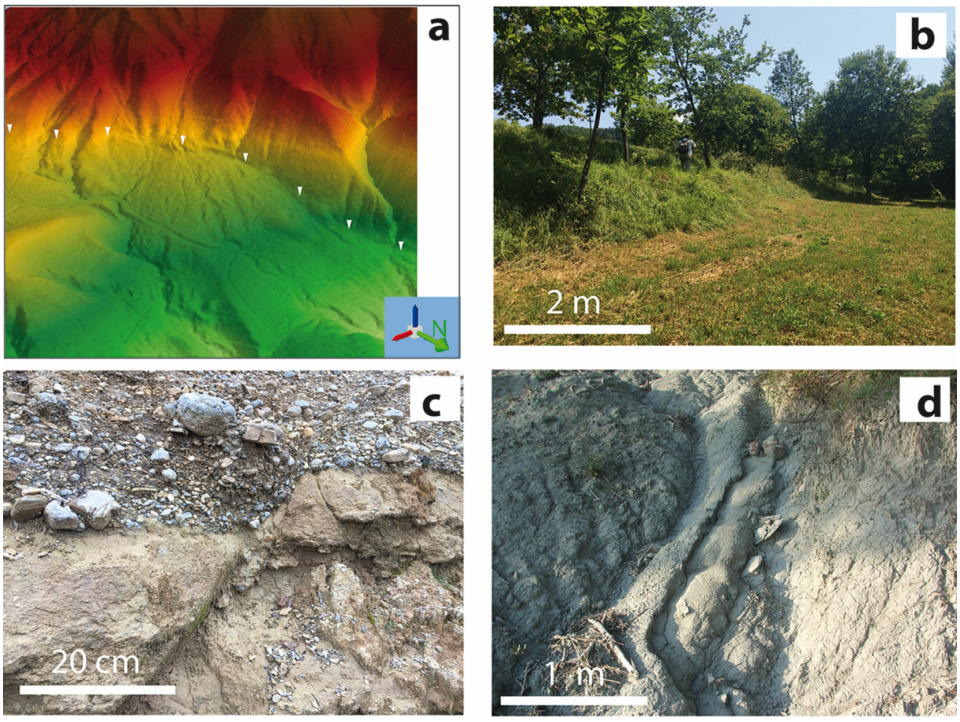

Figure 4. Evidence of Plio-Quaternary faulting and deformation: (**a**) LiDAR-derived DTM showing the fault scarp offsetting a Late Pleistocene–Holocene alluvial fan along the Mulazzo Fault in the structural domain SD2 (Lunigiana). This site has been recently trenched for paleoseismological studies [68,69]; (**b**) fault scarp offsetting Late Pleistocene alluvial fan deposit along the southernmost splay of the Corfino Fault, in structural domain SD3 (Garfagnana); (**c**) normal fault offsetting the Late Villafranchian Olivola Conglomerates, in structural domain SD2 (Lunigiana); (**d**) Ruscinian Sarzanello–Caniparola sands and clay tilted by the Sarzana–Carrara fault, in the northern part of the West Alpi Apuane Fault system in the structural domain SD6 (La Spezia–lower Lunigiana). Locations of these sites are shown in the Figures related to the different SDs.

From a structural point of view, domain SD2 represents a ~40 km long, NW-trending graben with a maximum width of about 15–20 km in the south of the basin and decreasing northwestwards (Figure 3). The graben is bounded by antithetic high-angle normal fault systems overprinting a polydeformed contractional thrust stack and a later system of low-angle extensional detachments [50,68,69].

To the east, the west-dipping faults form 3 subparallel, NW-trending, closely spaced (a few km) fault systems running over a total length of more than 40 km along the entire upper Lunigiana extensional domain [58,70,71]. From east to west these systems are the Groppodalosio–Compione–Comano, the Arzengio–Bagnone, and the Mocrone–Licciana strands (Figure 3). Each of these fault systems is segmented laterally into a few major segments (whose names constitute the system names), most of 10–15 km length. Some of these segments have been studied in detail. The Groppodalosio fault segment runs over ~18 km from the Passo del Righello (west of Cisa Pass) to the southwest of Mt. Sillara. It has a strike from N 130° to N 170° and shows a steep dip and normal slip kinematics with a cumulative displacement of ~400 m near Groppodalosio. The Compione–Comano fault segments [59,66,70–74] form a ~20 km long fairly connected strand dipping 60–70° to the SW. The Groppodalosio and Compione–Comano fault segments show a right-stepping "en échelon" pattern suggestive of a left-lateral component of slip on the whole system, in addition to the dominant normal one. On the Compione–Comano fault zone, a cumulative vertical displacement of more than 2000 m has been inferred from surface and subsurface data [50,59,75]. This suggests that the cumulative vertical slip decreases from south to north along the whole Groppodalosio–Compione–Comano fault system. The Late Pleistocene era

conglomerates appear vertically displaced across of the Groppodalosio and the Compione–Comano faults [59,66], attesting for their slip motions in the last 100 kyrs.

The Arzengio–Bagnone and the Mocrone–Licciana faults extend over a total length of ~25 km. Their largest cumulative vertical displacement is estimated at ~600 m [59,72,73]. The Arzengio fault is considered to have been active mainly in the pre-Middle Pleistocene times [59,66,67]. The Mocrone–Licciana Fault, which is closest to the graben axis, has a maximum throw of ~400 m. It is taken to have been active during and after the Middle Pleistocene [66,67]. Two small adjacent faults, Fivizzano and Minucciano, have been suggested to be inactive since the Middle Pleistocene [66].

The antitethic NE-dipping fault system that bounds the graben to the west includes the Coloretta–Parana–Podenzana–Tendola and the Arzelato–Mulazzo–Tresana–Aulla fault zones [50,59,73,74]. The former has a total length of about 35 km, while each segment is about 10–15 km long. The maximum cumulative vertical throw, ~700 m, is observed in the northernmost part of the fault system, where a dip-slip normal kinematics and a Late Pleistocene, possibly Holocene activity are inferred [59,73].

The Arzelato–Mulazzo–Tresana–Aulla fault system bounds the upper Lunigiana graben (Figures 3 and 4a). In its northern part, its normal dip-slip kinematics are attested by various indicators (some close to Mulazzo), while a cumulative vertical displacement of ~1000 m is observed. The fault system has been suggested to be active in the Holocene [59, 66,74], which paleoseismological trenching has confirmed recently [68,69].

Both the Coloretta–Parana–Podenzana and the Arzelato–Mulazzo–Tresana–Aulla faults have their strike changing from the NW–SE to W/NW–E/SE toward their southernmost termination, where they seem to connect to the North Apuane Fault System (described below, Fosdinovo–Tenerano–Marciaso–Aiola–Equi Terme Faults in Figure 3).

Recent geomorphic analysis have been locally performed in the upper Lunigiana [66,73] with the aim to estimate the cumulative fault throws and their variations along strike, the fault segmentation pattern, and the possible linkages among the fault segments and systems [59,66,68]. Among others, these studies have derived late Quaternary throw rates in the range of 0.4–0.8 mm/year, in fair agreement with displacement rates suggested in earlier works from geological studies (Table S1).

4.3. Structural Domain SD3: The Garfagnana

Structural domain SD3 includes the Garfagnana, an intramontane depression where the Serchio valley is developed (Figure 6). The Plio-Quaternary stratigraphic units exposed in the area (Figure 2) are characterized by:

(a) Basal, fine-grained lithofacies, mainly clays and silty clays locally interbedded with coarse-grained conglomerates alternating to thin beds and lenses of sands and organic-rich horizons [56,76–78]. Thin dark grey paleosols are also present, at different levels of the clayed–sandy sediments and related to local emersion of the depositional area [56,79–81]. These dominantly fine-grained basal lithofacies, called Fornaci di Barga clays, have a maximum thickness of 170–200 m (inferred in exploration wells near Pieve di Fosciana and Barga [56]). According to the paleontological contents, the formation is attributed to Middle–Late Pliocene; in particular the lower portion could be assigned to the Ruscinian–Early Villafranchian, while the upper portion could reach the Late Middle Villafranchian [56,79–81];

(b) Barga conglomerates, which are dominated by coarse-grained lithofacies with subordinate silty to sandy interbeds mainly distributed into the lowermost portion where organic-rich horizons also are observed. In contrast with the conglomerates interbedded within the Fornaci di Barga clays, the Barga conglomerates are formed more than 50% by Mesozoic carbonate clasts sourced from both the unmetamorphic and the metamorphic Tuscan units. The thickness of the sequence ranges from 70 to ~170 m and can be referred to the Late Villafranchian, based on its correlation with the similar Olivola conglomerates [79–81].

Commonly, the sedimentary record of the Villafranchian sequences is interpreted to attest to a depositional environment with a transition from lacustrine to fluvial [76–78]. More recently, however, some authors [79,80] have related its formation to an alluvial

system with NW–SE flow direction developed in a humid subtropical climate regime, followed by the development of a gravel bed-load braided system.

(c) Post-Villafranchian deposits are represented by: (i) Macigno-derived conglomerates; and (ii) terrace alluvial deposits, with decreasing altitude above the present riverbed [66,77,78].

The distribution of the Villafranchian and post-Villafranchian deposits along the present Garfagnana and their internal structural setting document significant syn- and post-Villafranchian [66,81–83] vertical movements and deformations related to the activity of fault systems described hereafter (Figures 5 and 6).

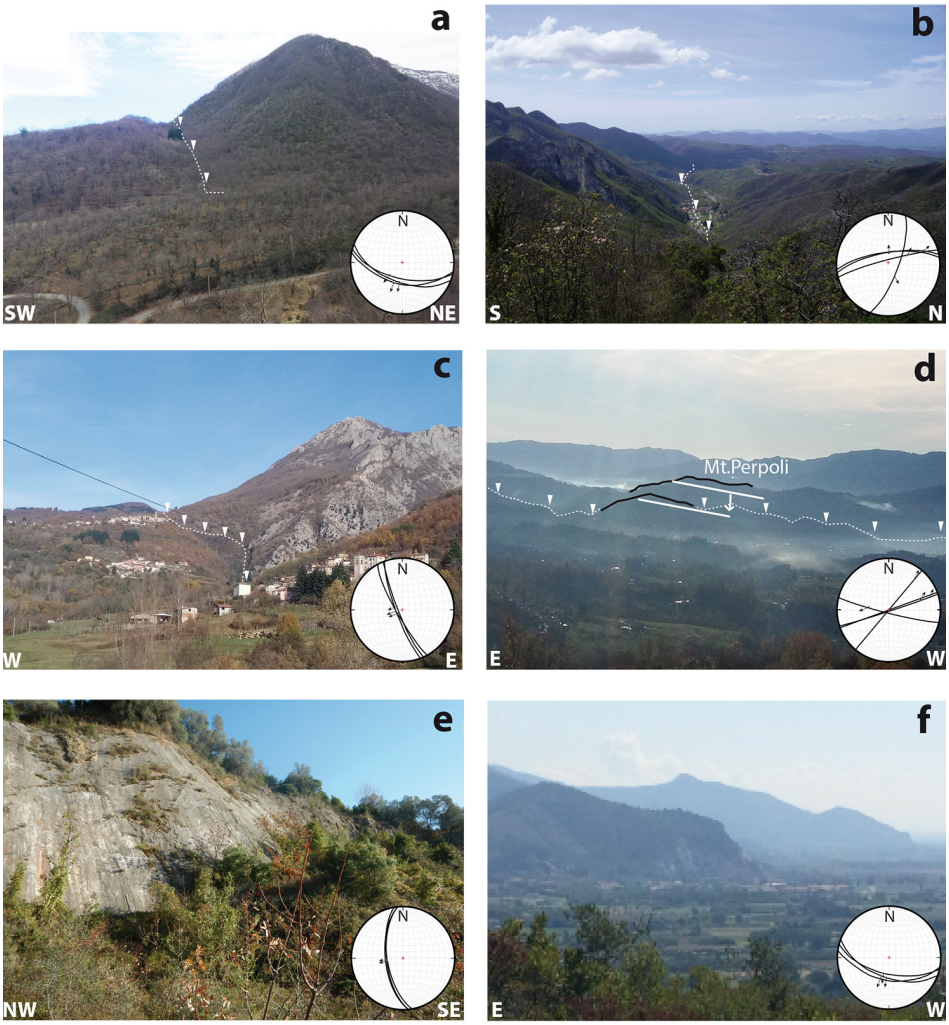

Figure 5. (**a**) Panoramic view (toward N/NW) of the Compione Fault (structural domain SD2). (**b**) Panoramic view (toward W/SW) of the Aiola–Equi Terme fault part of the North Apuane Fault System. The village in the valley is Equi Terme, epicentral area of the 2013 Lunigiana earthquake. Photo taken from the road to Ugliancaldo Village, epicentral area of the 1837 Alpi Apuane earthquake; (**c**) Corfino fault in structural domain SD3. (**d**) Monte Perpoli morphostructural high in SD3. White line indicates the base of the Late Pleistocene deposits in the hanging wall and footwall of the North Mt. Perpoli fault. The latter is taken to have produced the 2013 Garfagnana earthquake. (**e**) Pietrasanta fault (SD5), central southern segment of the West Alpi Apuane fault, the major bounding fault of the Viareggio basin. (**f**) Basin and range landscape forming the western boundary of the Pisa plain (southernmost part of the structural domain SD5). Stereonets show microtectonic measurements we made on the faults (minor fault planes and slickenslides) (Schmid net, lower hemisphere).

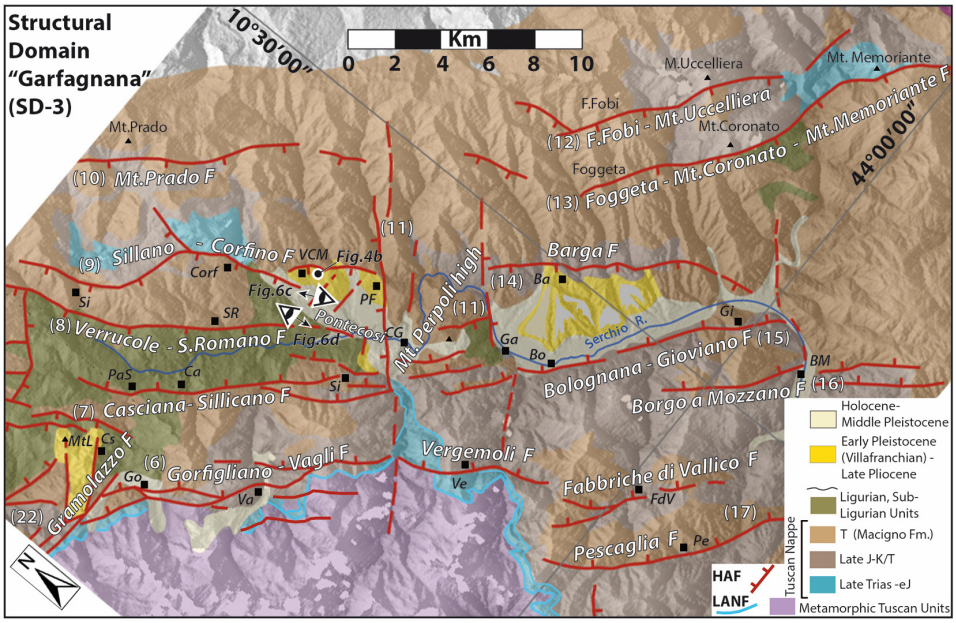

Figure 6. Main fault systems and geology in structural domain SD3 (Garfagnana). The map is derived from [56,57,77,84] and our work. Fault identification numbers are as reported in Table S1. HAF: steep normal faults; LANF: low-angle detachment faults; Ba: Barga; BM: Borgo a Mozzano; Bo: Bolognana; Ca: Casciana; CG: Castelnuovo Garfagnana; Cs: Castagnola; Corf: Corfino; Ga: Gallicano; Gi: Gioviano; Go: Gorfigliano; MtL: Mt. Lupacino; PaS: Piazza al Serchio; Pe: Pescaglia; PF: Pieve Fosciana; Si: Sillicano; SR: San Romano; Va: Vagli; VCM: Villacollemandina; Ve: Vergemoli.

From a structural point of view, domain SD3 represents a ~30 km long, NW-trending graben with a maximum width of about 20 km in the SE, slightly decreasing northwestward (Figure 6). As with SD2, it is bounded by antithetic steep normal fault systems overprinting the contractional thrust stack and a set of low-angle extensional detachments, mainly located at the base and within the Tuscan unmetamorphic unit [50]. SD3 is divided in its center by the Mt. Perpoli high (between Castelnuovo Garfagnana and Barga), a normal fault bounded horst trending subperpendicular to the graben faults (Figure 5d). This transverse relief divides SD3 into two subdomains, Garfagnana North and Garfagnana South.

The Garfagnana North subdomain is bounded to the East by three west-dipping fault systems: the Verrucole–S. Romano, the Sillano–Corfino, and the Mt. Prado systems. Each fault forming any of these systems is 10–15 km long. The Verrucole–S. Romano Fault has a total vertical throw of ~400 m, with offset recorded in the Late Pleistocene Macigno-rich conglomerates [56,66,82]. The fault also offsets by ~18 m more recent alluvial terraces toward its southern prolongation represented by the Pontecosi fault [66,82,83].

The Sillano–Corfino fault (Figures 4b and 5c) shows slickensides that are interpreted to suggest a right-lateral component of slip in addition to the dominant normal one [74]. The total vertical offset of the Corfino fault is ~600 m, with deformation in the Villafranchian and post-Villafranchian deposits. Smaller vertical displacement of ~250 m is measured in its southern part [66,77,82,83], between Villa Collemandina and Castiglione Garfagnana (Figure 4b).

The M. Prado fault, close and at the straddle with the orographic divide, is a ~10 km long structure with a maximum cumulative vertical offset of ~300 m and evidences of post Last Glacial Maximum (LGM) activity [56,66].

To the west, the graben is bounded by two major NE-dipping normal fault systems, the Gorfigliano–Vagli and the Casciana–Sillicano systems. Both seem to continue beyond the transverse Mt. Perpoli high, in the form of the NE-dipping Vergemoli–Fabbriche di Vallico–Pescaglia and the Bolognana–Gioviano–Borgo Mozzano fault zones, respectively.

All these fault systems are segmented laterally, with each identified fault being one of these segments, 10–15 km long.

The Casciana–Sillicano and Bolognana–Gioviano faults bound the present graben axis. Along these faults, the cumulative vertical displacement increases from north to south, up to ~400 m west of Castelnuovo Garfagnana (Casciana–Sillicano Fault), and up to 1.5 km across the Tuscan units around the Gallicano village (Bolognana–Gioviano Fault). There, the Barga conglomerates are vertically offset by about 39 m [56,66].

In the Garfagnana South subdomain, the eastern border faults are represented by the west-dipping Foce a Fobi/Mt. Uccelliera and the Foggeta–Mt.Coronato–Mt.Memoriante normal faults. The former is ~18 km long and shows well-expressed topographic scarps [56,66]. The latter is a ~20 km long structure with more than 300 meters of cumulative vertical displacement that bounds the Mesozoic carbonatic inlier of the Lima Valley to the west [84].

Further west, the Barga fault closely bounds the graben. It is a segmented fault about 10 km long with a NW–SE trend that bends to nearly N–S toward its southern termination close to Borgo a Mozzano, where it abuts against the east-dipping Gioviano fault. The distribution of the Late Pleistocene alluvial deposits has been related to the activity of the Barga Fault [56,66,73,77].

The Mt. Perpoli high that divides SD3 is bounded to the north and south by NE-trending faults with an oblique dextral and normal slip locally well constrained in bedrock minor faults [66,72,83] (Figure 5d). Deformation of Villafranchian and post-Villafranchian deposits has been described across the faults [56,66,82,83], which document a minimum of ~250 m of vertical displacement during Plio-Quaternary and ~150 m in the Middle Pleistocene–Holocene. An intermittent historical activity of the Pieve di Fosciana sinkhole-related lake has been related to the activity of the Mt. Perpoli faults [85].

4.4. The Lunigiana and Garfagnana Linkage Zone

The northern part of domain SD3 includes an area where a structural linkage seems to occur between the major fault systems of domains SD2 and SD3 (Figure 7). In this linkage zone, the oldest Plio-Quaternary continental deposits are largely eroded, although they are observed in three major exposures close to Canova–Ceserano and S. Terenzo in the Lunigiana and between Minucciano and Piazza al Serchio in Garfagnana [57,59,86]. The oldest levels, represented by clays, sands, and mainly polygenic conglomerates [56,57,86], may be compared with the Aulla clay–Collecchia conglomerates in Lunigiana and with the Fornaci di Barga fm. in Garfagnana [56,57,60]. These deposits are unconformably covered by ~200 m thick Mg-dominant conglomerates (called M. Lupacino conglomerates), which are considered of Early Villafranchian age [57], or more likely Late Villafranchian–Middle Pleistocene from correlation with similar deposits in Lunigiana and Garfagnana [58,60] (Figure 2). The original flat erosive base of these Plio-Quaternary deposits is vertically displaced by about +30, +50, and +500 m at the Canova–Ceserano, S. Terenzo, and Castagnola–M. Lupacino exposures, respectively, compared to similar deposits exposed in Lunigiana and Garfagnana.

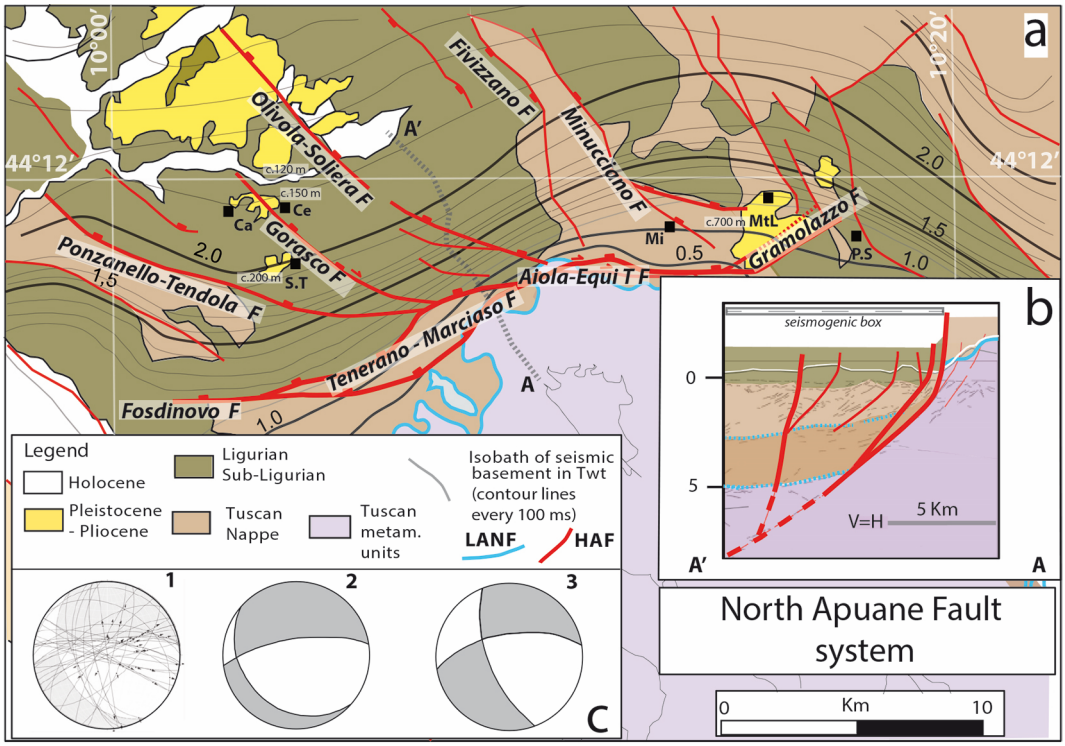

Figure 7. Lunigiana–Garfagnana linkage domain between SD2 and SD3, with the surface and subsurface architecture of the North Apuane Fault System. (**a**) Simplified tectonic and geological map of the Lunigiana–Garfagnana linkage domain (location in Figure 3) with breakthrough surface faults (Fosdinovo–Tenerano–Marciaso–Aiola–Equi T.–Gramolazzo and splays). HAF: steep normal faults; LANF: low-angle detachment faults. The contours are depths (in TWT) of the seismic basement identified in the seismic profiles, down to 5000 m; they image the North Apuane fault plane in the subsurface, as shown in (**b**). Numbers c.000 m indicate the elevation of the base of Plio-Pleistocene deposits. (**b**) Interpreted seismic section across the North Apuane fault (ENI: Equi Terme–Monti migrated line; more details in [50]). (**c**) Fault data (main fault planes and secondary faults with striations) showing kinematics of Aiola–Equi Terme Fault (1) and fault slip data inversion, PT kinematic diagrams (2, 3). All kinematic indicators attest to an oblique slip, both normal and right-lateral. Ca: Canova; Ce: Ceserano; Mi: Minucciano; Mt.L: M. Lupacino; P.S: Piazza al Serchio; S.T: S. Terenzo Monti.

The Lunigiana and Garfagnana linkage domain is related to the North Apuane fault system (Figures 3, 6 and 7). This fault zone, trending about ENE, is the most prominent structure in the morphology (Figure 5b) and the best constrained both at the surface and in the subsurface (Figure 7), thanks to Eni seismic lines [50,66,87]. In the seismic profiles, the North Apuane fault is well imaged down to a ~5 km depth (~2s in TWT, Figure 7b). Dipping by ~50° toward about the north, it separates a metamorphic footwall domain (Apuane metamorphic units in subsurface) from the unmetamorphic cover units of the nappe stack [50,87]. At the surface, the fault extends over more than 30 km long and is divided into three connected, ~10 km long segments: from west to east: the ~E–W trending Fosdinovo fault, the central ~NE-trending Tenerano–Marciaso fault, and the ~E–W trending, Aiola–Equi Terme fault. Its total vertical slip is 2–3 km.

The Aiola–Equi Terme fault shows clear evidence of recent activity, such as bedrock fault scarps, triangular facets, and hydrothermal springs along the fault trace (Figure 5b) [17,66,87–89].

The overall architecture of the North Apuane fault zone and adjacent faults suggests that the Ponzanello–Tendola, Gorasco, and Olivola–Soliera faults are secondary splay faults of the major North Apuane fault. Altogether, these secondary faults form a large horsetail at the western termination of the North Apuane fault zone, in keeping with its right-lateral component of slip (Figure 7c). To the east, the Gramolazzo fault may also be a secondary fault connected to the North Apuane fault, although this has to be better

investigated. It displaces Plio-Quaternary deposits and a set of alluvial Late Pleistocene-Holocene terraces [86], which attests to its recent activity.

4.5. Structural Domain SD4: Lucca–Mt.Albano

Structural domain SD4 has been described as the "Montecarlo basin" [90–94] filled with up to ~2000 m of Neogene to Quaternary continental and marine stratigraphic sequences (exposed at surface and revealed in exploration wells; Figure 8).

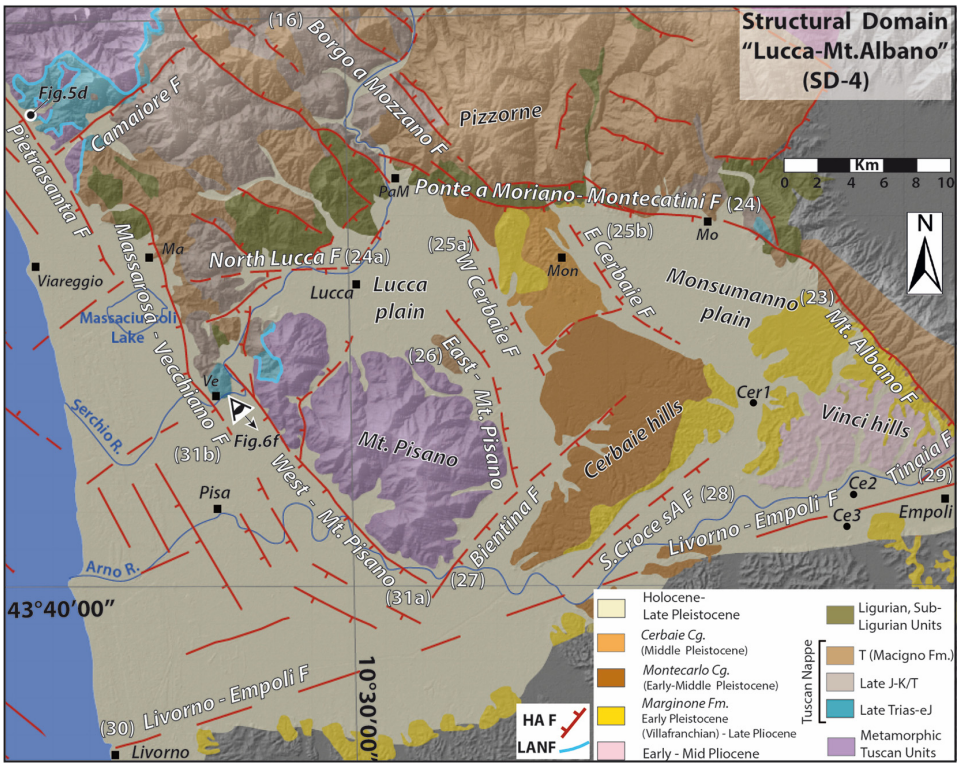

Figure 8. Major faults and geology in structural domain SD4 (Lucca–Mt. Albano). The map is derived from [92–94] and our work. Fault identification numbers as reported in Table S1. HAF: steep normal faults; LANF: low-angle detachment faults; Cer1: Cerbaie well; Ce2, Ce3: Certaldo wells; Ma: Massarosa; Mo: Montecatini; PaM: Ponte a Moriano; Ve: Vecchiano.

More precisely, SD4 includes two sub-basins, the Lucca and the Monsumanno plains, bounded by the hills of Montecarlo–Le Cerbaie and of Vinci. The basal terms of the filling sequence (Figure 2) are only known in subsurface at the Cerbaie 1 and Certaldo 2–3 boreholes, and tentatively referred to Late Miocene [90]. They consist of fluvio-lacustrine marls, clay and silty sands.

Their thickness is about 600 m in the Certaldo 2 and 3 boreholes, while the levels pinch out northward as documented in the Cerbaie 1 borehole. In outcrops, the lowermost terms are represented by the Marginone Fm. [90,91], which is formed by clays, silty clays, and sands locally associated with conglomerates. Fossil remnants and sedimentological features [92,95] document a transitional environment related to an alluvial plain grading southward to a marine environment. With a maximum thickness of ~400 m, the Marginone Fm. is dated to the Late Pliocene to Early Pleistocene (Early to Late Villafranchian) [95,96], although a possible Ruscian age has been suggested based on the presence of mammal remnants (*Alephis lyrix*) in its northermost part [92].

The overlaying Montecarlo conglomerates dominantly consist of a red gravelly deposit composed of quartzites and phyllites mainly sourced from the Triassic Verrucano Formation of the close Mt. Pisano. The unit, with a maximum thickness of 150–200 m, can be attributed to late Early Pleistocene, and is unconformably overlain by the Cerbaie Formation (Figure 2),

which displays the same composition as the Montecarlo Formation, although with a finer clast size.

The Cerbaie Formation, with a maximum thickness of 20–30 m, is dated at the Middle Pleistocene through a regional correlation with deposits cropping out on the southern side of the Arno Valley and containing a tuff layer radiometrically dated at about 0.5 Ma [91,93,95–98].

From a structural point of view, SD4 represents a rhomb-like graben (Figure 8). To the south it is bounded by the ENE-trending Livorno–Empoli fault, and to the east by the Mt. Albano west-dipping normal fault. While that fault extends over 20 km with a NNW-strike, it bends anticlockwise at its northern termination so as to form the WNW-trending Ponte a Moriano–Montecatini normal fault. The connection between the two NNW- and WNW-trending normal faults suggest oblique slip on both of them, left-lateral on the Mt. Albano fault and right-lateral on the Ponte a Moriano–Montecatini fault. The Mt. Albano fault seems to extend further south beyond the Livorno–Empoli Fault (Figure 1).

The western boundary of SD4 is marked by the east Mt. Pisano Fault, which is well defined in the subsurface [93] along the eastern side of Mt. Pisano. The interior of the SD4 fault-bounded basin is also dissected by a few faults, mainly the west- and east-dipping Cerbaie normal faults, which bound the Montecarlo–Cerbaie horst in the center of the basin. A few other faults (Bientina, S. Croce sull'Arno, and Tinaia) are inferred in the south of the basin from subsurface data [90,93,94,99], possibly connected to the Livorno–Empoli fault. Although the tectonic studies of the SD4 basin faults are still few, the available works show that the cumulative vertical displacement on the Mt. Albano fault is about 1000 meters in its northern part (around Monsummano–Montecatini), including ~250 m and at least ~150 m of vertical slip since the Early-Middle Pliocene and the Gelasian, respectively [94]. Southeast of the Cerbaie and Vinci hills, "erosional" scarps may represent the expression of the subsurface S. Croce sull'Arno and Tinaia faults [91–93]. Their post-Middle Pleistocene vertical displacement is estimated at ~110 m [91–94].

The WNW-trending Ponte a Moriano–Montecatini normal fault steps to the left in the western part of the basin, resulting in the south-dipping, ~E-W-trending North Lucca normal fault. The left-stepping arrangement of the two normal faults suggests a right lateral component of slip along the whole transverse fault system. The activity of this northern basin-bounding fault system is recorded in the Plio-Quaternary deposits where deformation postdating the Late Pliocene is well documented, as well as in the morphotectonic evolution of the footwall domain represented by the reliefs of Le Pizzorne [78,92,94].

4.6. Structural Domain SD5: The Viareggio Basin

Structural domain SD5 includes the northernmost of the Tuscany and Northern Tyrrhenian Neogene basins [30,31,50,100]. It is made of an onshore part with the coastal plains of Versilia and Pisa and of an offshore domain with a basin-depocenter west of Viareggio (Figure 9). The coastal plains of Versilia and Pisa are formed by Quaternary deposits mainly sourced from the major rivers, Magra, Serchio, and Arno, and their tributaries. The offshore Viareggio basin is known thanks to industrial seismic profiles and exploration wells offshore and onshore, which described a Neogene–Quaternary sedimentary filling up to ~3500 m thick [30,31,46,47]. According to [30,100], the sedimentary sequence starts with 300 m of marine clay and sandstone (Seq. 2+3 of [30,100]) considered to be Late Messinian by [30]. The Pliocene succession shows a thickness of about 1500 m and is subdivided into two sequences (Seq. 4 and 5) from seismic facies and unconformities [47,100,101]. The succession is mainly formed by outer neritic marine clay associated with sandy layers. The following Quaternary deposits include ~600 m of open marine to littoral-brackish alternations of clay and sand (Seq. 6a) with inclined and well-defined reflectors indicating a westward prograding sandy mouth-bar related to the development of the paleo-Arno river. Deposits related to a marine ingression define the bottom of an uppermost, ~100 m thick sequence (Seq. 6b) referred to the Middle Pleistocene–Holocene. This upper sequence is formed by marine to brackish sands associated with gravel layers and covered by 40 m thick clays.

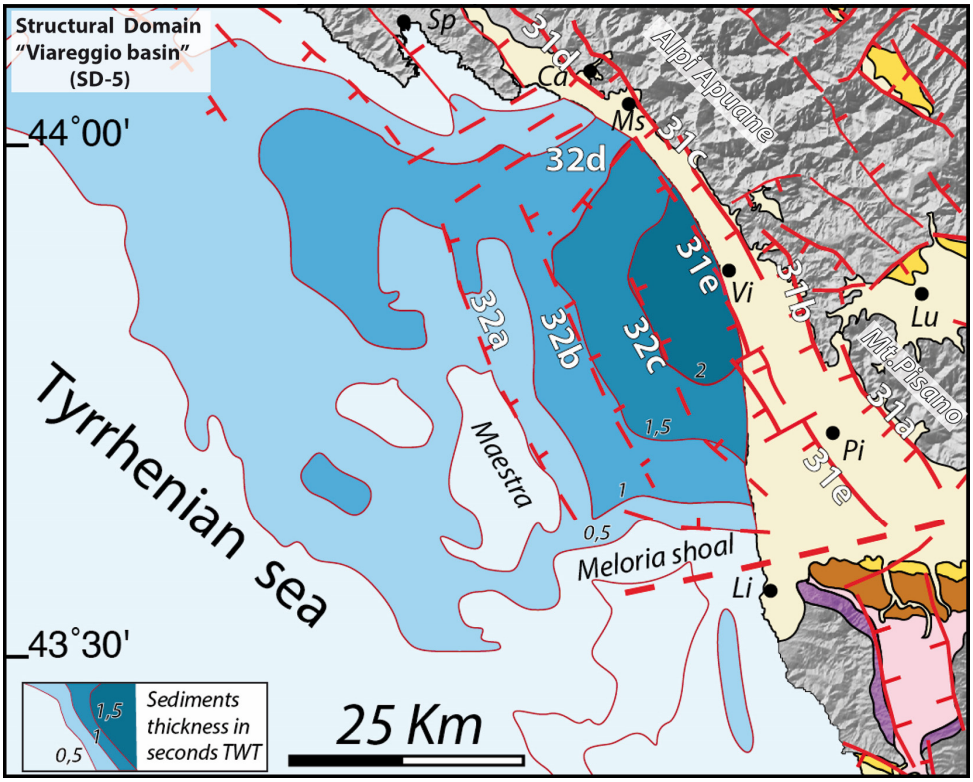

Figure 9. Main fault systems and geology in structural domain SD5 (Viareggio basin). Fault identification numbers are as reported in Table S1. Offshore sediment thickness after [30,31]. Ca: Carrara; Lu: Lucca; Li: Livorno; Ms: Massa; Pi: Pisa; Sp: La Spezia; Vi: Viareggio.

From a structural point of view, the Viareggio basin is an asymmetric, NNW-elongated graben, about 70 km long and 35–40 km wide (Figures 1 and 9). It is bounded to the north by submarine highs shaped by ~E–W trending faults offshore, Marina di Massa and Marina di Carrara, and to the south by the ENE-trending Meloria Shoal fault, which is the western offshore segment of the Livorno-Empoli fault. To the west, a submarine high, Maestra, forms the structural boundary of the basin, whereas to the east, the basin margin is made of a series of closely-spaced, west-dipping, steep normal faults that are part of the West Apuane Fault System (Figure 9). Seismic images and surface geology document the asymmetry of the basin controlled by the southwest-dipping master faults forming the West Apuane Fault System [50,87,99–102]. The relationships between faults and the sedimentary infill document deformation with total vertical offsets of more than 3500 m on the West Apuane system, and of ~200 m since the Middle Pleistocene. They provide evidence of activity of both the west- and east-dipping faults in Early Pliocene and Middle Pleistocene [100,101,103,104]. Although most of the available industrial seismic profiles do not have sufficient resolution to identify fault offsets within the Late Pleistocene–Holocene deposits, a few displacements are locally documented [46,105–107].

The kinematics of basin-margin high-angle faults is well constrained in some of the exhumed segments observable at the surface, as the Pietrasanta fault (Figures 5e and 8).

Close to Pisa, in the Mt. d'Oltre Serchio, a kilometer-wide relay zone between two NNW normal faults shows fault scarps up to 10 m high, likely formed in the Late Pleistocene–Holocene [103–105].

4.7. Structural Domain SD6: La Spezia–Lower Lunigiana

Structural domain SD6 is an on-land/offshore domain shaped by the Vara Valley–lower Lunigiana tectonic depression in which the Vara and the lower course of the Magra flow (Figure 10). The western promontory of La Spezia and the Vezzano–Pta. Bianca reliefs bound the depression. Continental stratigraphic sequences are scatterly observed in this

domain, and are especially known in the northwest near Sesta Godano, and along the eastern flank of the lower Lunigiana, from S. Stefano Magra to Sarzana [58,106–109]. Small sedimentary remnants between Sesta Godano and La Spezia [55,105,108] mark a paleohydrographic setting with record of the paleo-Vara now captured by the Magra river [55,108] (Figure 10).

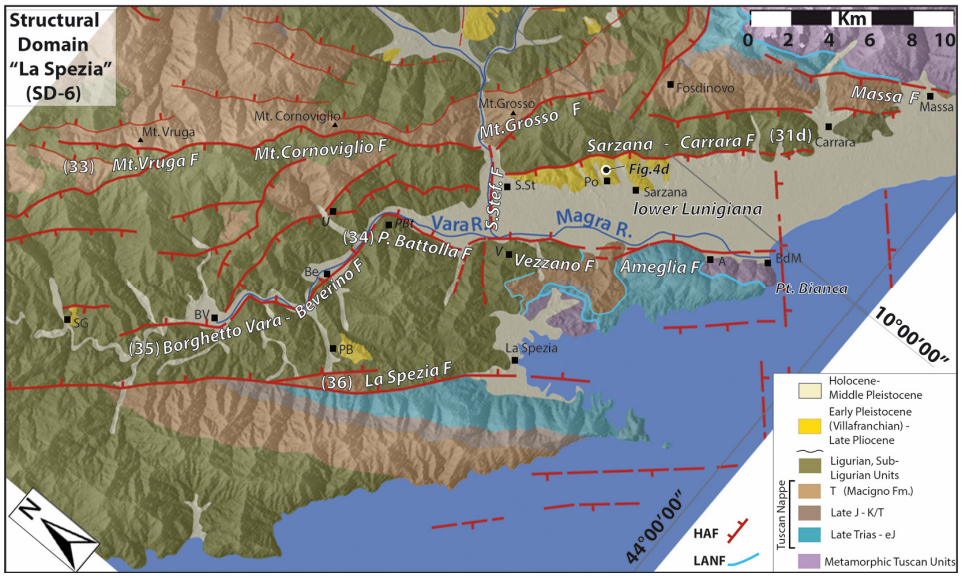

Figure 10. Main fault systems and geology in the structural domain SD6 (La Spezia–lower Lunigiana). The map is derived from [58,107] and our work. Fault identification numbers are as reported in Table S1. HAF: steep normal faults; LANF: low-angle detachment faults; A: Ameglia; BdM: Bocca di Magra; Be: Beverino; BV: Borghetto Vara; PB: Pian di Barca; PBt: Piano Battolla; Po: Ponzano Magra; SG: Sesta Godano; S.St: Santo Stefano Magra; U: Usurana; V: Vezzano.

The deposits of the lower Magra valley are related to a former Neogene–Quaternary "Sarzana basin" [58,107,108] associated with a continental sequence exploited in the past for clays and lignite deposits and containing rich flora and mammal remnants, and the object of investigations since the mid-19th century [107,109]. The sequence includes:

(a) Basal fine-grained lithofacies, mainly formed by clays and silty clays interbedded by thin beds and lenses of sand and lignite-bearing horizons grading and alternating upward with medium- to coarse-grained conglomerates. The dominantly fine-grained basal lithofacies, called Sarzanello–Caniparola clays [58,107–109], has been documented in the old mines around Caniparola and in less visible outcrops along the Albachiara creek south of Sarzanello [106,108,109]. The thickness of this unit is ~40 m and its depositional environment has been considered as related to lacustrian–palustrian in transition to a fluvio-deltaic setting developed in subtropical to temperate conditions. The paleontological contents allowed, with some debate, an attribution to the Early Pliocene, with its lower portion assigned to the Ruscinian age [108,109].

(b) Ponzano Magra clays and conglomerates, which are dominated by coarse-grained lithofacies with subordinate silty to sandy interbeds and fine-grained clay lithofacies mainly distributed in the lowermost portion, where organic-rich horizons are also present. In a quarry close to Ponzano Magra, the fine-grained lithofacies were used for industrial pottery until the mid-1980s. The Ponzano Magra clays and conglomerates, with a thickness of ~120 m [58,106,107], have been related to an alluvial plain environment and are characterized by a paleontological content which allows their dating to the Early–Middle (?) Villafranchian [61,106–109].

(c) Darma–Faggiada conglomerates, which are mainly formed by polygenic coarse-grained conglomerates associated with sands and silty-sand layers locally observable in fining-upward sequences. This unit is interpreted as related to alluvial fans resting

unconformably on top of the Ponzano Magra conglomerates. From relative chronology evidence, the unit is suggested of Middle–Late Villafranchian age [58,106–109].

(d) Fan deposits and alluvial terraces. The oldest of these units, collectively called the "lower Val di Magra system" [107], includes alluvial terraces and related fan deposits mainly observable in the eastern flank of the lower Magra valley (between S. Stefano di Magra and Sarzana). The sequences are represented by polygenic unsorted gravels and boulders with minor sands and clays, and are referrable to an evolving braided fluvial system and lateral fans. The oldest of this group of deposits, which may be found at about 50 m above the present Magra river, is well developed between nearby Santo Stefano di Magra and is related to an early stage of development of the present drainage system [107,109]. Collectively these units are attributed to the Middle–Late Pleistocene. The recent alluvial terraces and alluvial deposits are related to the present-day Magra–Vara river system and include two levels of terraces formed by conglomerates, sands, and silts. The oldest of these deposits have been dated to the Late Pleistocene–Holocene, while the youngest are of the Bronze and Iron Ages (due to the presence of a human-made "Statua Stele" found during sand quarrying near Sarzana [107]).

The deposits of Sesta Godano include conglomerates grading to coarse- to fine-grained sands interbedded with clay and silty clays. The sequence has a thickness of about 60 m and is related to a lacustrine–alluvial depositional system [58,107]. Pollen contents allowed its dating to the Early Villafranchian [106,108,109]. Noteworthy are the scattered coarse-grained deposits, mainly conglomerates and sands, observable NW of La Spezia in Pian di Barca surroundings. These deposits are interpreted as related to the confined alluvial systems [58,106] of Pliocene–Early Villafranchian age [58,107,108]. They thus attest to a past drainage of the paleo-Vara river flowing to the proto-La Spezia Gulf before its diversion toward the present-day course track [58].

The central graben—lower Lunigiana—of domain SD6 is bounded by antithetic normal fault systems (Figure 10). Overall, the width of the fault-bounded graben decreases from SE to NW. To the east, the major west-dipping Sarzana–Carrara fault, the northermost part of the West Apuane Fault System, extends over ~25 km from Carrara to S. Stefano di Magra, where it steps to the right to continue through the Mt. Grosso–Mt. Cornoviglio–M. Vruga fault [50,58,60]. The step has developed so that the fault system is intersected by a NE-trending short fault, the S. Stefano Magra fault. From the step toward the northwest, the Sarzana–Carrara fault splays into a network of curved normal faults, forming a sort of horsetail at the northern end of the Sarzana–Carrara fault. This horsetail suggests a left-lateral component of slip on the main NW-trending Sarzana–Carrara fault, in addition to its dominant normal one.

To the west of the graben, the east-dipping, NW-trending bounding normal fault system includes La Spezia fault, about 20 km long, and the Piano Battolla–Vezzano–Ameglia fault on the eastern side of the Punta Bianca promontory. With a total length of about 40 km, the Piano Battolla–Vezzano–Ameglia fault bends counterclockwise in its northern section, likely to connect the La Spezia fault.

The Quaternary vertical displacements on the Sarzana–Carrara fault exceed 700 m, as recorded in tilted lower levels of the "Sarzana Basin" [50,58,72,107,110], and are estimated to ~75 m during Mid-Pleistocene–Holocene. Deformations of Holocene alluvial terraces are also documented across the Ameglia–Piana Battolla fault [72,107,109].

5. Geodetic Data, and Historical and Instrumental Seismicity

5.1. Geodetic Data

We used GPS data recorded in 1998–2020 by continuous Global Navigation Satellite System (GNSS) stations operating in Italy and surroundings, along with GPS data collected in repeated temporary campaign measurements during the RETREAT project [25] in the northern Apennines, to calculate new horizontal velocity and strain-rate fields.

We processed the data following the same procedures as described in [111], to which we refer for more technical details. The main result of our GPS data processing was a set

of ground surface velocities, represented in Figure 11 relative to a fixed Eurasia reference frame [25,112]. The discrete velocities at each station, weighted by their uncertainties, were used to estimate a continuous velocity field, and its spatial gradients, using the multiscale method described in [113,114]. Figure 11 also shows the total strain-rate field (i.e., the second invariant of the strain-rate tensor), defined as the square root of the sum of squares of all its components, along with the horizontal principal strain axes (grey arrows). The diverging and converging arrows thus represent the directions of extensional and contractional deformation, respectively.

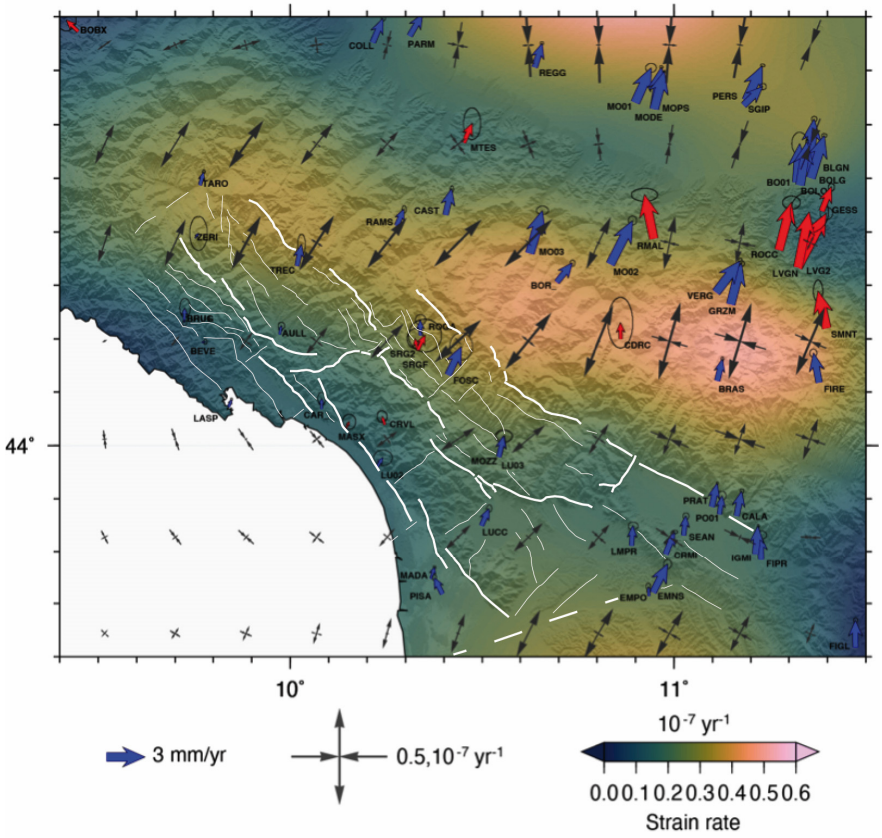

Figure 11. Horizontal GPS velocity field (blue and red vectors are continuous and campaign stations, respectively, with 95% confidence error ellipses) and total strain-rate field (color scale). The diverging and converging grey arrows show the axes of the principal strain rates, indicating extensional and contractional deformation, respectively.

Beyond the general characteristics of the velocity and strain fields, reported in earlier works [25,112], several interesting features were revealed.

First, surface velocities and strain rates abruptly changed across two zones trending about NW–SE: in the southwestmost part of the area, they increased significantly across a curved line that roughly coincided with the westernmost major fault systems of the SD2 and SD3 domains; whereas, further to the northeast, they decreased significantly across a curved line that runs in the Apennines northern flank, about 30–50 km east of the SD2 and SD3 easternmost fault systems. These pronounced changes might result from the current locking of active faults. In the region of concern here, this provides further support for the seismogenic activity of the westernmost SD2 and SD3 normal faults.

Another observation was the existence of a ~E-W narrow zone north of the Firenze graben, where the strain vectors suggest a strike-slip deformation. The zone roughly extends in the eastern prolongation of the ~E-W North Lucca–Ponte a Moriano–Montecatini fault zone that bounds the SD4 basin to the north. This is consistent with this fault zone, which currently has a right-lateral component of slip.

5.2. Historical and Instrumental Seismicity Within the Investigated Areas

The studied area is dominated by shallow earthquakes of low to moderate magnitude and normal to oblique focal mechanisms [1,2,4,27,115–118]. Figure 12 reports instrumental earthquakes with magnitude Mw >1 and historical earthquakes derived from the CPTI15 v.3 catalog [35,37]. Although instrumental and historical seismicity is widespread throughout the study area, only two seismogenic sources (in Lunigiana and Garfagnana, our SD2 and SD3 domains) are included in the national database of seismogenic areas. Figure 12 shows, however, that clusters of recent seismicity and historical earthquakes did occur in all the structural domains in the region of interest. Structural domain SD2 shows shallow crustal earthquakes, with hypocenter depths $\leq$ ~10 km, and focal mechanisms attesting to normal or oblique slips [116,117]. It is noteworthy that historical seismicity in this area includes different earthquakes with an estimated magnitude Mw > 5 (Figure 12c); among them, the "Val di Taro" (1545, Mw ~5.2) and "Bagnone" (1903, Mw ~5.3) events. Similar to upper Lunigiana, SD3 (Garfagnana) is an active seismic region, even though the distribution of instrumental seismicity is quite heterogeneous. Like in Lunigiana, the hypocenters are shallow ($\leq$10 km) and earthquakes have both extensional and oblique-slip kinematics. Leaving aside the 7 September 1920 earthquake (Mw ~6.5), which will be discussed below, at least five historical earthquakes with severe damages have been reported in Garfagnana [35,37] (Figure 12c): the "1740 Piastroso"(Mw ~5.2), the "1746 Barga" (Mw ~5), the "1902 Barga"(Mw ~4.9), the "1919 Piastroso" (Mw ~4.9), and the "1939 Vagli"(Mw ~4.9) earthquakes. The other structural domains described in this study show an instrumental seismicity less dense and of smaller maximum magnitudes (Mw < 3.5) than those recorded in the SD2 and SD3 domains. However, in all domains there is a significant seismicity, including clusters and/or alignments of epicenters, both onland and offshore (Figures 12 and 13). It is worthy to report here the offshore events that occurred along and off the coast of Pisa and Viareggio in 2013. Some occurred in clusters, which superimpose fairly well to the surface traces of some of the major faults we described earlier (Figure 13). Cross-sections across these faults and clusters support that the former may be the sources of the earthquake clusters (Figure 13). This confirms that the bounding faults of the Viareggio basin are currently active, as those north of SD4 and east of SD6. The focal mechanisms are too few to derive any significant information, but they confirm that earthquakes on NNW-trending faults have normal or normal and left-lateral slip.

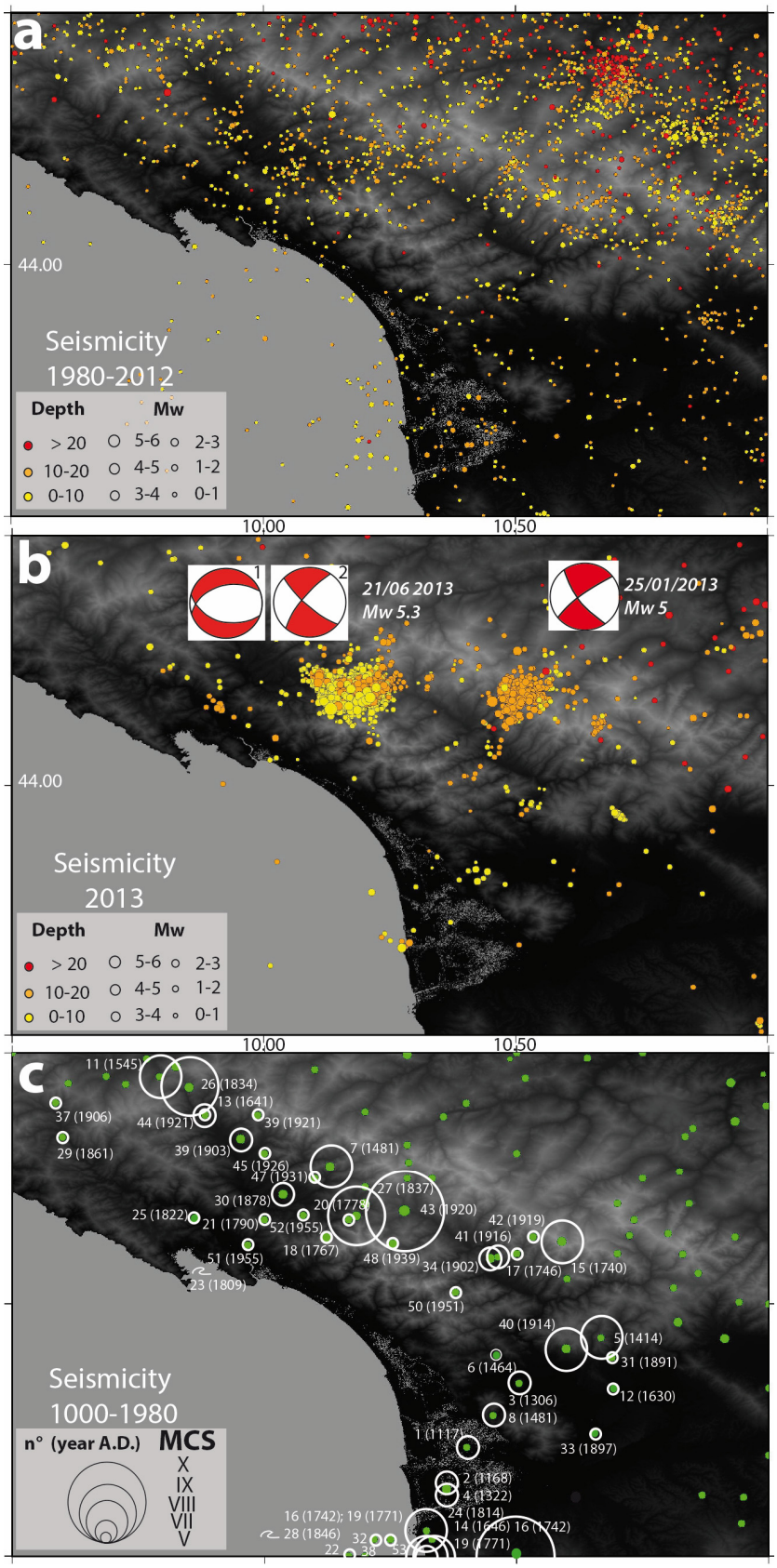

Figure 12. Seismicity in the studied area (instrumental and historical). (**a**) 1982–2012; (**b**) 2013; (**c**) historical moderate to large earthquakes (intensities greater than V) reported from 1000 to 1980 (from CPTI15-DBMI15 catalogs). Identification numbers are the same as those reported in Table S2.

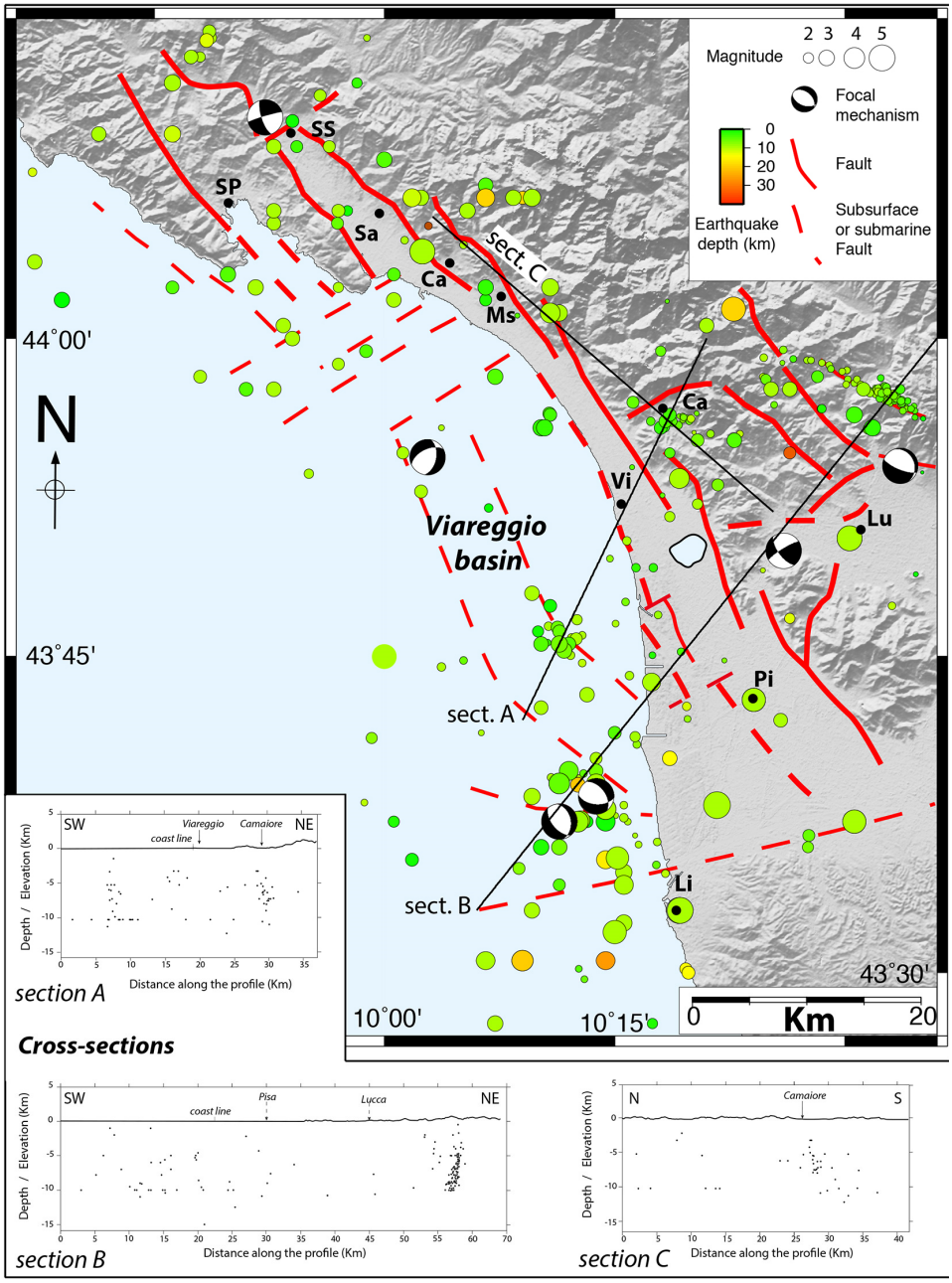

Figure 13. Faults and seismicity (1980–2013) in the Viareggio basin and surroundings. Focal mechanisms are from the INGV archive [2,32].

At least 11 historical moderate earthquakes with significant damages occurred within the structural domains SD4, SD5, and SD6 (Table S2): the 1168 "Pisa" (Mw ~4.5), the 1322 "Pisa"(Mw ~4.5), the 1414 "Villa Basilica" (Mw ~5.2), the 1481 "San Giuliano Terme" (Mw ~4.5), the 1630 "Pescia" (Mw ~4.5), the 1891 "Villa Basilica" (Mw ~4.5), the 1814 "Livorno" (Mw ~5.1), the 1861 "Varese Ligure" (Mw ~4.6), the 1897 "lower Val d'Arno" (Mw ~4.6), the 1914 "Ponte a Moriano" (Mw ~5.8), and the 1955 "Sarzana" (Mw ~4.5) earthquakes. Furthermore, an important earthquake occurred in the Viareggio–Pisa area in 1117 that caused large damages [37]. The significant magnitudes of these earthquakes attest that they ruptured fault lengths of kilometer scales. Altogether, these earthquake records thus confirm that at least several of the faults we have described in the region are currently active and seismogenic.

5.3. The 2013 Seismic Activity

During 2013, a series of seismic events occurred within the investigated area, soon after the end of the Emilia 2012 seismic sequence [4,33,74]. The 2013 events affected domain SD3 (Garfagnana) in January and the transition zone between SD2 and SD3 in June and August. A few other events occurred in the plain of Pisa and in the close offshore area, as well as in the lower Val di Magra (SD6) in April, June, and October (Figures 12 and 13).

On January 25 at 3:48 p.m., an earthquake with Mw 4.8 occurred in mid-Garfagnana at a depth of ~15 km (Figure 12b). The main shock was followed by about 300 aftershocks in the following days, with magnitudes that rarely exceeded Mw 3 [32]. The distribution of the aftershocks roughly draws a NE–SW trend, and the aftershocks migrated away from the main shock toward the NE. The location of the main shock and of the aftershocks appears unrelated to the two seismic sources recognized in the area by the DISS project [16]. The focal mechanisms suggest right-lateral slip on a NE–SW-trending plane or a left-lateral slip on a NW–SE-trending plane. As the cluster of January 2013 geometrically fits the area of the transversal, NE-trending fault zone (Mt. Perpoli high and related faults) that divides SD3 into two parts, the event provides support to the current activity of this fault zone.

On 21 June 2013 (10:33 UTC), an earthquake of Mw 5.2 hit southern Lunigiana, with its epicenter close to Monzone (Figures 1 and 12b). The main event was preceded by a foreshock on June 15 (Mw 3.4), and was followed by more than 2450 aftershocks, 4 of them having a magnitude Mw $\geq$ 4 and 27 with Mw $\geq$ 3 [32]. The data show that most aftershocks extended NE from the epicenter [4] (Figure 12b). INGV calculated two solutions for the focal mechanism of the main shock, with the one noted as (2) in Figure 12b being the best constrained. Both solutions are consistent with a N–S extension, while the best constrained mechanism suggests a normal left-lateral or a normal right-lateral slip on a NW- or NE-trending plane, respectively. The seismic source was initially constrained through the measurement of the coseismic surface deformation field with DInSAR interferometry, which defined a rupture on a normal fault dipping NNW by about 50° [119]. Refined results were later presented based on a combination of DInSAR and seismological data and hypocenter relocation [120]. These identified the source as a ~N 70° E striking normal fault, ~45° NNW-dipping fault with a main dip-slip mechanism, but combined with a small right-lateral strike-slip component [120]. This is consistent with our observations on the transverse faults.

The year 2013 was also marked by a series of small earthquakes throughout western Tuscany and eastern Liguria. While these earthquakes are sparse, some form clusters coinciding with the traces of some of the faults identified in the western flank of the Alpi Apuane, including offshore in the Viareggio basin, but also with the transversal NE–SW-trending faults offshore of SD6 (Figures 10 and 13).

6. The 1920 Mw ~6.5 Fivizzano Earthquake: Hypothesis on its Fault Source

On 7 September 1920 at 05:55, the area between southern Lunigiana and Garfagnana (SD 2 and SD3) was struck by a devastating earthquake with an estimated Mw of 6.4–6.5 [35,37].

The mainshock was preceded by some foreshocks on the previous day, and was followed by aftershocks that lasted until August 1921 [38]. The earthquake induced a vast area of severe damages throughout Lunigiana and Garfagnana and their surroundings, over an area of about 160 km^2 (Figure 14). The mainshock was felt up to the Côte d'Azur in southern France, Aosta in northwestern Italy, the Friuli region in the northeast, and south of Perugia in central Italy [38].

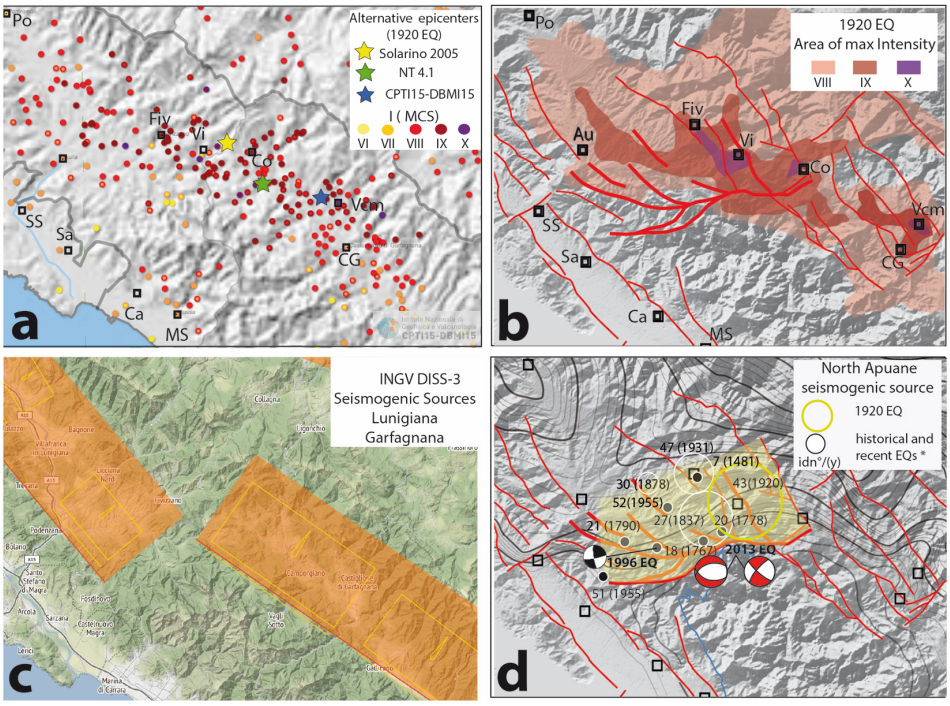

Figure 14. (**a**) Macroseismic field of the 1920 Fivizzano earthquake. MCS intensities are those of the database in [37], while epicentral positions are derived from different works (see legend). (**b**) Area of maximum intensity of the 1920 Fivizzano earthquake [35,37]. (**c**) Recognized seismogenic source according to DISS 3 [16]. (**d**) North Apuane Fault System architecture in surface and subsurface, with location of historical and recent earthquakes *. Light yellow represents the seismogenic source we inferred from Figure 7.

From the interpretations of the macroseismic field (Figure 14a) (which in some zones reached I 10 MCS) [37,38], different causative faults were proposed as the source of the 1920 Fivizzano earthquake. Among them, the most commonly proposed faults are the NW-trending, ~10 km long Minucciano fault in Lunigiana (SD2, Figure 3) and the NW-trending, ~15 km long Casciana–Sillicano fault in Garfagnana (SD3, Figure 6), which are among the seismogenic faults recognized in the national hazard map [16,17,116,117]. As a matter of fact, in the area between Lunigiana (SD2) and Garfagna (SD3) different historical earthquakes with Mw > 4 have been reported [37] (Figure 12c): the 1481 "Fivizzano" (Mw ~5.5), the 1767 "Monzone" (Mw ~5.3), the 1790 "Tendola" (Mw ~4,9), the 1837 "Alpi Apuane" (Mw ~5.8), and the 1878 "Olivola" (Mw ~5.1) earthquakes. Moreover, the epicenter of the 15 October 1995 Mw 4.9 earthquake [116–118,121], as that of the 21 June 2013 earthquake, are located in the same zone. Figure 14d shows the surface projection of the North Apuane Fault System that we described earlier (Figure 7). We suggest that this source may account for some of the recorded historical and instrumental events, and moreover, that its rupture produced the 1920 earthquake. As the North Apuane Fault System forms the northern termination of the NNW-trending, east-dipping westernmost faults of SD3, we hypothesize that the earthquake ruptured both the northern part of the NNW trending faults (Gorfigliano–Vagli or Casciana–Sillicano faults; Figure 6), and its ending oblique North Apuane fault. Coseismic slip might have been greater on this ending oblique fault, as observed elsewhere, such as in the 1999 Mw 7.6 Chichi earthquake [122]. Therefore, while some NNW-trending faults of the SD3 domain likely ruptured in the 1920 earthquake, we suggest that the ~E-W North Apuane fault extending at the northern tip of the SD3 NNW faults also ruptured during the earthquake, and actually likely produced the largest slips and ground accelerations [49,66,74,87]. This hypothesis will of course need to be validated by future fieldwork analyses.

7. Discussion

We have provided a review of most available knowledge on Cenozoic geology/stratigraphy, faulting, seismicity, and current surface strain in the inner northwest Apennines. This compilation allows us to discuss two major issues.

7.1. Fault Distribution and Evolution

Our work shows that the region of study is densely dissected by large faults of 10 to 40 km lengths. The dominant faulting trends NW–NNW, and has normal slip, however with an additional component of left-lateral slip. The faults are steep and commonly combine in conjugate pairs of antithetic faults bounding grabens. Figure 15 presents a simplified map of the principal grabens with their sedimentary Plio-Quaternay filling in yellow. These grabens are disconnected from each other or nested within one another, and their width is narrowing northwestward. Furthermore, collectively, they form an overall area that tapers northwestward. Graben tapering has been described elsewhere and shown to result from the propagation of extensional faulting in the direction of graben narrowing [123]. This architecture might thus suggest the northwestward propagation of extensional faulting in this part of the Apennines. Such a northwestward propagation of extensional faulting has already been proposed in earlier works [5,124]. It is consistent with the northwestward decrease of the total vertical slip along most of the major NW–NNW normal faults, indicative of faults becoming younger in the northwestward direction [125]. Furthermore, we note that the total vertical slips accommodated on the graben-bounding faults decrease overall from west (~3.5 km in the Viareggio basin) to east, where total slip on the easternmost faults is half that on the westernmost faults. This might suggest a migration of extensional strain over time from west to east, in addition to the northwestward propagation.

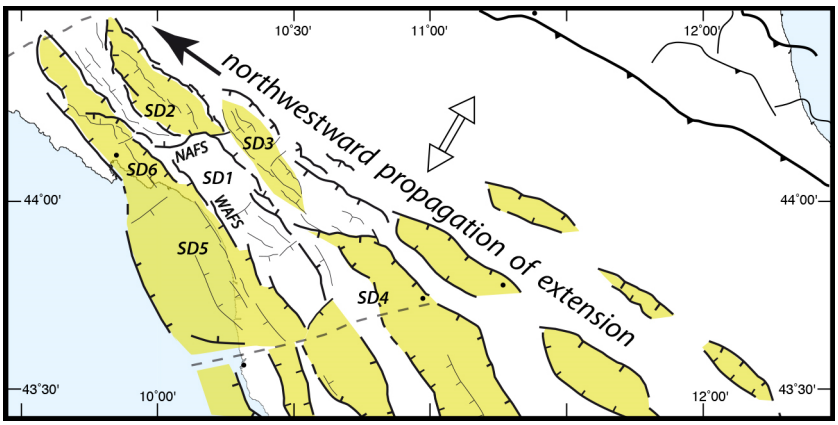

Figure 15. Simplified map of major extensional fault systems in the inner northwest Apennines. Principal grabens are represented, with their sedimentary Plio-Quaternary filling in yellow. The NW–NNW fault systems are suggested to have propagated northwestward in the few last million years. SD: structural domain; NAFS: North Apuane Fault System; WAFS: West Apuane Fault System.

Although most NW–NNW faults are likely to interact (as shown in central Italy, e.g., [5,126]), they are disconnected, sometimes en échelon disposed, so that each principal fault is at most 40 km long, and more generally 10–15 km.

Another fault set exists in the region, trending almost perpendicular to the dominant NW–NNW normal faults. The origin of these transverse faults is not yet fully investigated. As similar ENE faults exit throughout most of Italy, they might likely arise from structural inheritance from earlier phases of deformation [127–130]. In the region of study, the most important of these ENE faults are the TAL and LEF, which may act at depth as major shear zones. They actually have a right-lateral component of slip. Some of these faults might be reactivated by the NW–NNW normal, left-lateral faults. This might be the case for the

North Apuane and the Mt. Perpoli faults. Being strongly oblique to the major NW–NNW west-dipping faults of the SD2 and SD3 domains, and located at their tips, they sustain extension due to the left-lateral component of slip on these principal NW–NNW faults.

More work is needed to confirm the fault organization and evolution suggested in Figure 15, and to validate whether this architecture results from the overall propagation of extensional faulting toward the northwest, along with a possible eastward migration of the strain locus. Whatever it is, the architecture of the faults depicted in this study markedly differs from the seismotectonic model proposed so far in [131], in which faulting would be mainly related to a major low-angle, east-dipping active detachment [47,131,132]. Rather, we show that faults are steep, paired in conjugate sets bounding grabens, and disconnected, although forming a kinematically coherent overall fault system.

7.2. Evidence for Recent Fault Activity and Implications for Seismic Hazard

One of the most important results of this work was to document that the majority of faults described in the study have been active over the Quaternary. Most show displacements post-800 ka, and in some cases clear slips across Late Pleistocene and Holocene deposits [59,66,69,72,83]. In addition, some of these faults show evidence of recent to current activity. Yet, most of these seismogenic faults are not considered in the national and local hazard evaluations. While most of the faults we identified are shorter than 35–40 km, they may have the potential to produce strong earthquakes. Most are indeed immature (as defined in [11]), and it has been shown that, while immature faults are shorter than more mature faults, they produce more energetic earthquakes (i.e., larger stress drops), generating greater displacements at depth and surface [11], and stronger ground motions [14]. Therefore, it is possible that some of the faults we identified can generate one to several meters of slip when they rupture, and large ground accelerations. Furthermore, immature faults tend to rupture in cascade, each of their major segments rupturing individually at successive times [5,11,126]. Such cascading earthquakes have been reported elsewhere in Italy on other similar normal faults (e.g., [5,126]). We have shown that most of the NW–NNW normal faults in northwest Apennines are segmented laterally in generally 3–4 major segments, each 10–15 km length. According to the available earthquake slip-length scaling laws [11], the rupture of one of such segments might produce up to 1–3 m of slip at the ground surface, likely accompanied with strong ground accelerations. As shown in Central Italy, such earthquakes might have a magnitude between 6 and 7, and can follow in close time successions [5,126].

Therefore, our study emphasizes that seismic hazard is significant in the inner northwest Apennines and should be considered [133,134], especially as the presence of thick, soft alluvial deposits in the Viareggio, Pisa, and lower Arno valleys [97,134] may lead to the amplification of ground movements and accelerations. The hazard might even be more complex as some of the seismogenic faults extend offshore where their dip-slip rupture might generate tsunamis, as already recorded in the past in La Spezia and Livorno [135]. Onland, the large vertical slips expected in the faults might trigger significant landsliding.

8. Conclusions

Using the rich information in the literature, along with field observations we made, we propose a reappraisal of the active fault identification and mapping in the inner northwest Apennines. We showed that faults active in Quaternary times are numerous in the region and dominated by NW–NNW antithetic normal faults bounding a series of disconnected grabens. Most of the faults show evidence of Quaternary activity up to the present time. Most of the faults identified in this work are thus likely seismogenic, i.e., potential sources of forthcoming earthquakes. The properties of the faults are such that these earthquakes are expected to be potentially large (Mw $\geq$ 6.0), to produce up to several meters of slip at the ground surface, and to possibly occur in temporal cascades. The seismic hazard is thus significant in the region, and even greater than expected if cascading earthquakes are the norm.

Therefore, our study calls for the need to evaluate in greater detail the recent activity and the earthquake potential of the many faults we identified as potentially seismogenic. We claim that the majority of them should be included in the Italian seismic hazard evaluation. We hope that our work will encourage the national and regional authorities to support the needed geological, tectonic, and seismological research studies in the inner northwest Apennines. These should include tectonic fault analysis with remote sensing and fieldwork, seismological recording and analysis, densification of the GPS network, paleoseismological trenching, and fault-scarp dating, among others. These future studies are critical to assess seismic hazard more accurately in the densely populated areas from La Spezia to Lucca–Pisa–Livorno, which presently have low seismic protection codes.

Supplementary Materials: The following are available online at https://www.mdpi.com/2076-3263/11/3/139/s1, Table S1: Fault systems, timing of activity, displacements, displacement rates, and related references; Table S2: Historical earthquakes in the investigated area based on the CPTI15 and CPTI-DBMI15 databases.

Author Contributions: Conceptualization, G.M., J.M., I.M.; validation, G.M., R.B., J.M., E.S., F.S., I.M.; formal analysis, G.M., R.B., J.M., I.M., E.S., F.S.; investigation, G.M., F.S., A.B., G.P., A.L., T.G., L.A., L.P.; resources, G.M., A.B., G.P., S.G.; data curation, A.B., G.P., S.G.; writing—original draft preparation, G.M., I.M.; writing—review and editing, G.M., I.M.; visualization, S.G.; project administration, G.M.; funding acquisition, G.M., F.S., E.S., R.B., I.M. All authors have read and agreed to the published version of the manuscript.

Funding: This research was funded by Ateneo funds from Pisa University, FIL grants from Parma University, and ANR projects QUAKonSCARPS and FAULTS_R_GEMS. The APC was funded by an Ateneo grant from Pisa University.

Acknowledgments: We thank the two reviewers Paolo Galli and Stefano Mazzoli for their detailed comments that greatly helped us to improve our manuscript.

Conflicts of Interest: The authors declare no conflict of interest.

References

1. Chiarabba, C.; Jovane, L.; Di Stefano, R. A new view of Italian seismicity using 20 years of instrumental recordings. *Tectonophysics* **2005**, *395*, 251–268. [CrossRef]
2. Pondrelli, S.; Salimbeni, S.; Ekström, G.; Morelli, A.; Gasperini, P.; Vannucci, G. The Italian CMT dataset from 1977 to the present. *Phys. Earth Planet. Inter.* **2006**, *159*, 286–303. [CrossRef]
3. Meletti, C.; Galadini, F.; Valensise, G.; Stucchi, M.; Basile, R.; Barba, S.; Vannucci, G.; Boschi, E. A seismic source zone model for the seismic hazard assesment of the Italian territory. *Tectonophysics* **2008**, *450*, 85–108. [CrossRef]
4. Scafidi, D.; Barani, S.; De Ferrari, R.; Ferretti, G.; Pasta, M.; Pavan, M.; Spallarossa, D.; Turino, C. Seismicity of Northwestern Italy during the last 30 years. *J. Seismolog.* **2015**, *19*, 201–218. [CrossRef]
5. Benedetti, L.; Manighetti, I.; Gaudemer, Y.; Finkel, R.; Malavieille, J.; Pou, K.; Arnold, M.; Aumaître, G.; Bourlès, D.; Keddadouche, K. Earthquake synchrony and clustering on Fucino faults (Central Italy) as revealed from in situ 36Cl exposure dating. *J. Geophys. Res.* **2013**, *118*. [CrossRef]
6. Schlagenhauf, A.; Manighetti, I.; Benedetti, L.; Gaudemer, Y.; Finkel, R.; Malavieille, J.; Pou, K. Earthquake supercycles in Central Italy, inferred from 36Cl exposure dating. *Earth Planet. Sci. Lett.* **2011**, *320*, 487–500. [CrossRef]
7. Galli, P. Recurrence times of central-southern Apennine faults (Italy): Hints from paleoseismology. *Terra Nova* **2020**. [CrossRef]
8. Galli, P.; Galadini, F.; Pantosti, D. Twenty years of paleoseismology in Italy. *Earth Sci. Rev.* **2008**, *88*, 89–117. [CrossRef]
9. Field, E.H. UCERF3: A new earthquake forecast for California's complex fault system. *Fact Sheet* **2015**. [CrossRef]
10. Wesnousky, S.G. Seismological and structural evolution of strike-slip faults. *Nature* **1988**, *335*, 340–342. [CrossRef]
11. Manighetti, I.; Campillo, M.; Bouley, S.; Cotton, F. Earthquake scaling, fault segmentation, and structural maturity. *Earth Planet. Sci. Lett.* **2007**, *253*, 429–438. [CrossRef]
12. Perrin, C.; Manighetti, I.; Ampuero, J.-P.; Cappa, F.; Gaudemer, Y. Location of the largest earthquake slip and fast rupture controlled by along-strike change in fault structural maturity due to fault growth. *J. Geophys. Res.* **2016**, *121*, 1–19. [CrossRef]
13. Stirling, M.W.; Wesnousky, S.G.; Shimazaki, K. Fault trace complexity, cumulative slip, and the shape of the magnitude-frequency distribution for strike-slip faults: A global survey. *Geophys. J. Int.* **1996**, *124*, 833–868. [CrossRef]
14. Radiguet, M.; Cotton, F.; Manighetti, I.; Campillo, M.; Douglas, J. Dependency of Near-Field Ground Motions on the Structural Maturity of the Ruptured Faults. *Bull. Seism. Soc. Am.* **2009**, *99*, 2572–2581. [CrossRef]

15. Chiaraluce, L.; Di Stefano, R.; Tinti, E.; Scognamiglio, L.; Michele, M.; Casarotti, E.; Cattaneo, M.; De Gori, P.; Chiarabba, C.; Monachesi, G.; et al. The 2016 Central Italy Seismic Sequence: A First Look at the Mainshocks, Aftershocks, and Source Models. *Seism. Res. Lett.* **2017**, *88*, 757–771. [CrossRef]
16. DISS Working Group. Database of Individual Seismogenic Sources (DISS), Version 3.2.1: A Compilation of Potential Sources for Earthquakes Larger than M 5.5 in Italy and Surrounding Areas. 2018. Available online: http://diss.rm.ingv.it/diss/ (accessed on 15 March 2021).
17. ITHACA Working Group. ITHACA (ITaly HAzard from CApable Faulting), A Database of Active Capable Faults of the Italian Territory. Version December 2019. ISPRA Geological Survey of Italy. Available online: http://sgi2.isprambiente.it/ithacaweb/Mappatura.aspx (accessed on 15 March 2021).
18. Elter, P. Introduction à la géologie de l'Apennin septentrional. *Bullettin Soc. Geol. Fr.* **1975**, *7*, 956–962. [CrossRef]
19. Carmignani, L.; Decandia, F.A.; Fantozzi, P.L.; Lazzarotto, A.; Liotta, D.; Meccheri, M. Tertiary extensional tectonics in Tuscany (Northern Apennines, Italy). *Tectonophysics* **1994**, *238*, 295–315. [CrossRef]
20. Jolivet, L.; Faccenna, C.; Goffé, B.; Mattei, M.; Rossetti, F.; Brunet, C.; Storti, F.; Funiciello, R.; Cadet, J.P.; D'Agostino, N.; et al. Midcrustal shear zones in postorogenic extension: Example from the northern Tyrrhenian Sea. *J. Geophys. Res.* **1998**, *103*, 12123–12160. [CrossRef]
21. Molli, G. Northern Apennines-Corsica orogenic system: An updated overview. Siegesmund, S.; Fügenschuh, B.; Froitzheim, N. Eds.; Tectonic aspects of the Alpine–Dinaride–Carpathian system. *Geol. Soc. Lond. Spec. Publ.* **2008**, *298*, 413–442. [CrossRef]
22. Elter, P.; Giglia, G.; Tongiorgi, M.; Trevisan, L. Tensional and compressional areas in the recent (Tortonian to present) evolution of the northern Apennines. *Boll. Geofis. Teor. Appl.* **1975**, *17*, 3–18.
23. Carminati, E.; Doglioni, C. Alps vs. Apennines: The paradigm of a tectonically asymmetric Earth. *Earth Sci. Rev.* **2012**, *112*, 67–96. [CrossRef]
24. Le Breton, E.; Handy, M.; Molli, G.; Ustaszewski, K. Post-20 Ma motion of the Adriatic plate—new constraints from surrounding orogens and implications for crust-mantle decoupling. *Tectonics* **2017**, *36*, 3135–3154. [CrossRef]
25. Bennett, R.A.; Serpelloni, E.; Hreinsdóttir, S.; Brandon, M.T.; Buble, G.; Basic, T.; Casale, G.; Cavaliere, A.; Anzidei, M.; Marjonovic, M.; et al. Syn-convergent extension observed using the RETREAT GPS network, northern Apennines, Italy. *J. Geophys. Res.* **2012**, *117*, B04408. [CrossRef]
26. Faccenna, C.; Becker, T.W.; Miller, M.S.; Serpelloni, E.; Willett, S. Isostasy, dynamic topography, and the elevation of the Apennines of Italy. *Earth Planet. Sci. Lett.* **2014**, *407*, 163–174. [CrossRef]
27. D'Acquisto, M.; Dal Zilio, L.; Molinari, I.; Kissling, E.; Gerya, T.; van Dinther, Y. Tectonics and seismicity in th Northern Apennines driven by slab retreat and lithospheric delamination. *Tectonophysics* **2020**, *789*. [CrossRef]
28. Mazzoli, S.; Santini, S.; Macchiavelli, C.; Ascione, A. Active tectonics of the outer northern Apennines: Adriatic vs. Po Plain seismicity and stress fields. *J. Geodyn.* **2015**, *84*, 62–76. [CrossRef]
29. Benedetti, L.; Tapponier, P.; Gaudemer, Y.; Manighetti, I.; Van der Woerd, J. Geomorphic evidence for an emergent active thrust along the edge of Po Plain: The Boni-Stradella Fault. *J. Geophys. Res. Space Phys.* **2003**, *108*, 2238. [CrossRef]
30. Mariani, M.; Prato, R. I bacini neogenici costieri del margine tirrenico: Approccio sismico-stratigrafico. *Mem. Soc. Geol. Ital.* **1988**, *41*, 519–531.
31. Bigi, G.; Cosentino, D.; Parotto, M.; Sartori, R.; Scandone, P. Structural model of Italy, Sheets 1–6. Scale 1:500,000. *CNR Quad. Ric. Sci.* **1983**, *114*, 3.
32. Scognamiglio, L.; Tinti, E.; Quintiliani, M. Time Domain Moment Tensor (TDMT). *Ist. Naz. Geofis. Vulcanol. INGV* **2006**. [CrossRef]
33. Martelli, L.; Santulin, M.; Sani, F.; Tamaro, A.; Bonini, M.; Rebez, A.; Corti, G.; Slejko, D. Seismic hazard of the Northern Apennines based on 3D seismic sources. *J. Seism.* **2017**, *21*, 1251–1275. [CrossRef]
34. Picotti, V.; Pazzaglia, F.J. A new active tectonic model for the construction of the northern Apennines mountain front near Bologna (Italy). *J. Geophys. Res. Space Phys.* **2008**, *113*, B08412. [CrossRef]
35. Rovida, A.; Locati, M.; Camassi, R.; Lolli, B.; Gasperini, P. The Italian earthquake catalogue CPTI15. *Bull. Earthq. Eng.* **2020**, *18*, 2953–2984. [CrossRef]
36. Piccinini, D.; Chiarabba, C.; Augliera, P. Compression along the northern Apennines? Evidence from the Mw 5.3 Monghidoro earthquake. *Terra Nova* **2006**, *18*, 89–94. [CrossRef]
37. Guidoboni, E.; Ferrari, G.; Tarabusi, G.; Sgattoni, G.; Comastri, A.; Mariotti, D.; Ciuccarelli, C.; Bianchi, M.G.; Valensise, G. CFTI5Med, the new release of the catalogue of strong earthquakes in Italy and in the Mediterranean area. *Sci. Data* **2019**, *6*, 80. [CrossRef] [PubMed]
38. de Ferrari, R.; Ferretti, G.; Barani, S.; Spallarossa, D. Investigating on the 1920 Garfagnana earthquake (Mw=6.5); Evidences of site effects in Villa Collemandina (Tuscany, Italy). *Soil Dyn. Earthq. Eng.* **2010**, *30*, 1417–1429. [CrossRef]
39. Ghelardoni, R. Osservazioni sulla tettonica trasversale dell'Appennino Settentrionale. *Boll. Della Soc. Geol. Ital.* **1967**, *84*, 1–14.
40. Rosenbaum, G.; Agostinetti, N.P. Crustal and upper mantle responses to lithospheric segmentation in the northern Apennines. *Tectonics* **2015**, *34*, 648–661. [CrossRef]
41. Monteforti, B.; Raggi, G. Lineamenti strutturali fra l'alta Val di Vara e il Passo Cento Croci: Considerazioni sulla linea trasversale Val Taro-Val Parma. *Atti Soc. Toscana Sci. Nat. Mem.* **1980**, *87*, 275–284.
42. Bernini, M.; Vescovi, P.; Zanzucchi, G. Schema strutturale dell'Appennino Nord-Occidentale. *L'ateneo Parm. Acta Nat.* **1997**, *33*, 43–54.

43. Cerrina Feroni, A.; Martelli, L.; Martinelli, P.; Ottria, G.; Catanzariti, R. Carta Geologico-Strutturale dell'Appennino Emiliano-Romagnolo. Note Illustrative. Regione Emilia-Romagna Selca, Firenze. 2002. Available online: http://hdl.handle.net/11380/629938 (accessed on 15 March 2021).
44. Bernini, M.; Papani, G. Alcune considerazioni sulla struttura del margine appenninico emiliano tra lo Stirone e l'Enza (e sue relazioni con il sistema del Taro). *L'ateneo Parm. Acta Nat.* **1987**, *24*, 219–240.
45. Bortolotti, V. La tettonica trasversale dell'Appennino, I—La linea Livorno–Sillaro. *Boll. Soc. Geol. Ital.* **1966**, *85*, 529–540.
46. Bernini, M.; Boccaletti, M.; Moratti, G.; Papani, G.; Sani, F.; Torelli, L. Episodi compressivi neogenico-quaternari nell'area estensionale tirrenica. Dati in mare e a terra. *Mem. Della Soc. Geol. Ital.* **1990**, *45*, 577–589.
47. Argnani, A.; Bernini, M.; Di Dio, G.M.; Papani, G.; Rogledi, S. Stratigraphic record of crustal-scale tectonics in the Quaternary of the Northern Apennines (Italy). *Ital. J. Quat. Sci.* **1997**, *10*, 595–602.
48. Bernini, M.; Bertoldi, R.; Papani, G.; Vescovi, P. Evoluzione in regime compressivo del Bacino villafranchiano di Compiano (Parma). *Atti Ticinensi Sci. Terra* **1994**, *37*, 155–171.
49. Eva, E.; Ferretti, G.; Solarino, S. Superposition of different stress orientations in the western sector of the northern Apennines (Italy). *J. Seismol.* **2005**, *9*, 413–430. [CrossRef]
50. Molli, G.; Carlini, M.; Vescovi, P.; Artoni, A.; Balsamo, F.; Camurri, F.; Clemenzi, L.; Storti, F.; Torelli, L. Neogene 3-D Structural Architecture of the North-West Apennines: The Role of the Low-Angle Normal Faults and basement thrusts. *Tectonics* **2018**, *37*, 2165–2196. [CrossRef]
51. Piana Agostinetti, N. The structure of the Moho in the Northern Apennines: Evidence for an incipient slab tear fault? *Tectonophysics* **2005**, *655*, 88–96. [CrossRef]
52. Chiarabba, C.; Giacomuzzi, G.; Bianchi, I.; Piana Agostinetti, N.; Park, J. From underplating to delamination-retreat in the northern Apennines. *Earth Planet. Sci. Lett.* **2014**, *403*, 108–116. [CrossRef]
53. Abbate, E.; Balestrieri, M.L.; Bigazzi, G.; Norelli, P.; Quercioli, C. Fission-track datings and recent rapid denudation in northern Apennines, Italy. *Mem. Soc. Geol. Ital.* **1994**, *48*, 579–585.
54. Fellin, M.G.; Reiners, P.W.; Brandon, M.T.; Wüthrich, E.; Balestrieri, M.L.; Molli, G. Thermochronologic evidence for the exhumational history of the Alpi Apuane metamorphic core complex, northern Apennines, Italy. *Tectonics* **2007**, *26*, 26. [CrossRef]
55. Isola, I.; Mazzarini, F.; Molli, G.; Piccini, L.; Zanella, E.; Zanchetta, G.; Drysdale, R.; Hellstrom, J.; Woodhead, J.; Roncioni, A.; et al. New chronological constraints from hypogean deposits for late Pliocene to Recent morphotectonic history of the Alpi Apuane (NW Tuscany, Italy). *Geosciences* **2021**, *11*, 65. [CrossRef]
56. Puccinelli, A.; D'Amato Avanzi, G.; Perilli, N. *Note Illustrative Della Carta Geologica d'Italia, Scala 1:50.000, CARG Foglio 250 Castelnuovo Garfagnana ISPRA*; DREA: Pratovecchio, Italy, 2016; p. 167.
57. Conti, P.; Carmignani, L.; Massa, G.; Meccheri, M.; Patacca, E.; Scandone, P.; Pieruccioni, D. *Note Illustrative Della Carta Geologica d'Italia, Scala 1:50.000, CARG Foglio 249 Massa ISPRA*; Regione Toscana: Florence, Italy, 2020; p. 290.
58. Raggi, G. Neotettonica ed evoluzione paleogeografica plio-pleistocenica del bacino del Fiume Magra. *Mem. Della Soc. Geol. Ital.* **1985**, *30*, 35–62.
59. Bernini, M.; Papani, G. La distensione della fossa tettonica della Lunigiana nordoccidentale (con carta geologica alla scala 1:50,000). *Boll. Della Soc. Geol. Ital.* **2002**, *121*, 313–341.
60. Puccinelli, A.; D'Amato Avanzi, G.; Perilli, N. Note Illustrative Della Carta Geologica d'Italia, Scala 1:50.000, CARG Foglio 233 Pontremoli ISPRA. A.T.I.-S.El.CA.srl-L.A.C. Srl-System Cart srl. 2015, p. 127. Available online: https://arpi.unipi.it/handle/11568/781624#.YFIKYdwRW00 (accessed on 15 March 2021).
61. Azzaroli, A. The Villafranchian stage in Italy and the Plio-Pleistocene boundary. *Giorn. Geol.* **1977**, *41*, 61–79.
62. Bertoldi, R. Una sequenza palinologica di eta' rusciniana nei sedimenti lacustri basali del bacino di Aulla-Olivola (Val Magra). *Riv. Ital. Paleontol. Stratigr.* **1988**, *94*, 105–138.
63. Federici, P.R. Nuovi resti di vertebrato nel bacino fluvio-lacustre villafranchiano di Pontremoli (Val di Magra). *Boll. Mus. Stor. Nat. Lunigiana* **1981**, *1*, 71–74.
64. Bertoldi, R. Indagini palinologiche nel deposito fluvio-lacustre villafranchiano di Pontremoli (Val di Magra). *L'ateneo Parm. Acta Nat.* **1984**, *20*, 155–163.
65. Federici, P.R. La tettonica recente dell'Appennino: 2. Il bacino fluvio-lacustre di Pontremoli (alta Val di Magra) e sue implicazioni neotettoniche. *Gruppo Di Studio Del Quat. Padano. Quad.* **1978**, *4*, 121–131.
66. Di Naccio, D. Morphotectonic analysis of the Lunigiana and Garfagnana Grabens (Northern Italy): Implications for Active and Potentially Seismogenic Normal Faulting. Ph.D. Thesis, Università Degli Studi di Chieti-Pescara, Pescara, Italy, 2009; p. 97.
67. Moretti, A. Evoluzione tettonica della Toscana settentrionale tra il Pliocene e l'Olocene. *Boll. Soc. Geol. Ital.* **1992**, *111*, 459–492.
68. Piccardi, L.; Nirta, G.; Montanari, D.; Moratti, G.; Blumetti, A.M.; Di Manna, P.; Vittori, E.; Baglione, M.; Fabbroni, P. Geological Setting and First Paleosismological Data on the Mulazzo Fault (Lunigiana Basin, Northern Tuscany). GNGTS-2019 Volume Abstract. Session-S1, 108–112. 2019. Available online: www3.ogs.trieste.it/gngts/index.php/15-pagina-sessione-2019/75-2019-1-1 (accessed on 15 March 2021.).
69. Nirta, G.; Vittori, E.; Blumetti, A.M.; Di Manna, P.; Benvenuti, D.; Montanari, D.; Perini, M.; Fiera, F.; Moratti, G.; Baglione, M.; et al. Geomorphic and paleo seismological evidence of capable faulting in the Northern Apennines (Italy): Insights into active tectonics and seismic hazard of the Lunigiana basin. *Geomorphology* **2021**, *374*, 107486. [CrossRef]

70. Bernini, M.; Papani, G.; Dall'Asta, M.; Lasagna, S.; Heida, P. The upper Magra valley extensional basin: A cross section between Orsaro Mt. and Zeri (Massa province). *Boll. Della Soc. Geol. Ital.* **1991**, *110*, 451–458.
71. Argnani, A.; Barbacini, G.; Bernini, M.; Camurri, F.; Ghielmi, M.; Papani, G.; Rizzini, F.; Rogledi, S.; Torelli, L. Gravity tectonics driven by Quaternary uplift in the Northern Apennines: Insights from the La Spezia-Reggio Emilia geo-transect. *Quat. Int.* **2003**, *101–102*, 13–26. [CrossRef]
72. Pinelli, G. Tettonica Recente e Attiva nell'Appennino Interno a Nord Dell'arno: Una Revisione Delle Strutture e Delle Problematiche. Diploma Thesis, Università di Pisa, Pisa, Italy, 2013; p. 89.
73. Di Naccio, D.; Boncio, P.; Brozzetti, F.; Pazzaglia, F.J.; Lavecchia, G. Morphotectonic analysis of the Lunigiana and Garfagnana grabens (northern Apennines, Italy): Implications for active normal faulting. *Geomorphology* **2013**, *201*, 293–311. [CrossRef]
74. Bonini, M.; Corti, G.; Delle Donne, D.; Sani, F.; Piccardi, L.; Vannucchi, G.; Genco, R.; Martelli, L.; Ripepe, M. Seismic sources and stress transfer interaction among axial normal faults and external thrust fronts in the Northern Apennines (Italy): A working hypothesis based on the 1916–1920 time–space cluster of earthquakes. *Tectonophysics* **2016**, *680*, 67–89. [CrossRef]
75. Lucca, A.; Storti, F.; Molli, G.; Muchez, P.; Schito, A.; Artoni, A.; Balsamo, F.; Corrado, S.; Mariani, E.S. Seismically enhanced hydrothermal plume advection through the process zone of the Compione extensional Fault, Northern Apennines, Italy. *GSA Bull.* **2019**, *131*, 547–571. [CrossRef]
76. Calistri, M. II-Il Pliocene fluvio-lacustre della conca di Barga. *Mem. Soc. Geol. Ital.* **1974**, *13*, 1–21.
77. Dallan, L.; Nardi, R.; Puccinelli, A.; D'sAmato Avanzi, G.; Trivellini, M. Valutazione del rischio di frana in Garfagnana nella media valle del Serchio (Lucca). Carta geologica e carta della franosità degli elementi Sillano, Corfino, Fosciandora e Coreglia (scala 1:10,000). *Boll. Della Soc. Geol. Ital.* **1991**, *110*, 245–272.
78. Bartolini, C.; Bernini, M.; Carloni, G.C.; Costantini, A.; Federici, P.R.; Gasperi, G.; Lazzarotto, A.; Marchetti, G.; Mazzanti, R.; Papani, G.; et al. Carta neotettonica dell'Appennino settentrionale. *Note illustrative Boll. Della Soc. Geol. Ital.* **1982**, *101*, 523–549.
79. Landi, E.; Ravani, S.; Sarti, G.; Sodini, M. The Villafranchian deposits of the Castelnuovo Garfagnana and the Barga basins (Lucca, Tuscany, Italy): Facies analysis and paleoenvironmental reconstruction. *Atti Della Soc. Toscana Di Sci. Nat.* **2003**, *108*, 81–93.
80. Perilli, N.; Puccinelli, A.; Sarti, G.; D'Amato Avanzi, G. Villafranchian deposits of the Barga and Castelnuovo Garfagnana basins (Tuscany, Italy): Lithostratigraphy and sedimentary features. *IL Quat.* **2004**, *17*, 313–322.
81. Coltorti, M.; Pieruccini, P.; Rustioni, M. The Barga Basin (Tuscany): A record of Plio-Pleistocene mountain building of the Northern Apennines, Italy. *Quat. Int.* **2008**, *189*, 56–70. [CrossRef]
82. Puccinelli, A. Un esempio di tettonica recente nella Val di Serchio: Il sollevamento di Monte Perpoli. *Atti Della Soc. Toscana Di Sci. Nat. Mem. Ser. A* **1987**, *94*, 105–117.
83. Angeli, L. Tettonica Recente-Attiva Nella Media Garfagnana: Revisione Geologico-Strutturale e Problematiche di Microzonazione Sismica. Diploma Thesis, Università di Pisa, Pisa, Italy, 2018; p. 108.
84. Botti, F.; Daniele, G.; Baldacci, F. *Note Illustrative Della Carta Geologica d'Italia, Scala 1:50.000, CARG Foglio 251 Porreta, ISPRA*; System Cart: Roma, Italy, 2017; p. 193.
85. La Rosa, A.; Pagli, C.; Molli, G.; Casu, F.; De Luca, C.; Pieroni, A.; Avanzi, G.D. Growth of a sinkhole in a seismic zone of the northern Apennines (Italy). *Nat. Hazards Earth Syst. Sci.* **2018**, *18*, 2355–2366. [CrossRef]
86. Bartolini, C.; Bortolotti, V. Studi di geomorfologia e neotettonica. I—I depositi continentali dell'Alta Garfagnana in relazione alla tettonica Plio-Pleistocenica. *Mem. Soc. Geol. Ital.* **1971**, *10*, 203–245.
87. Molli, G.; Torelli, L.; Storti, F. The 2013 Lunigiana (Central Italy) earthquake: Seismic source analysis from DInSar and seismological data, and geodynamic implications for the northern Apennines. A discussion. *Tectonophys* **2016**, *668–669*, 108–112. [CrossRef]
88. Brozzetti, F.; Boncio, P.; Tinari, D.P.; Di Naccio, D.; Torelli, L. LANFs attive e relativi meccanismi di trasferimento alla terminazione settentrionale dell'Etrurian Fault System (Lunigiana–Garfagnana, Italia). *Rend. Della Soc. Geol. Ital.* **2007**, *4*, 164–165.
89. Molli, G.; Doveri, M.; Manzella, A.; Bonini, L.; Botti, F.; Menichini, M.; Montanari, D.; Trumpy, E.; Ungari, A.; Vaselli, L. Surface-subsurface structural architecture and groundwater flow of the Equi Terme hydrothermal area, Northern Tuscany Italy. *Ital. J. Geosci.* **2015**, *134*, 442–457. [CrossRef]
90. Ghelardoni, R.; Giannini, E.; Nardi, R. Ricostruzione paleogeografica dei bacini neogenici e quaternari nella bassa valle dell'Arno sulla base dei sondaggi e dei rilievi sismici. *Mem. Soc. Geol. Ital.* **1968**, *7*, 91–106.
91. Federici, P.R.; Mazzanti, R. L'evoluzione della paleogeografia e della rete idrografica del Valdarno Inferiore. *Boll. Soc. Geol. Ital.* **1988**, *5*, 573–615.
92. Dallan, L. Ritrovamento di Alephis lyrix nelle argille della serie lacustre di Montecarlo (Lucca) e considerazioni stratigrafiche sui depositi continentali dell'area tra il Monte Albano e il Monte Pisano. *Atti Soc. Toscana Sci. Nat. Mem. Ser. A* **1988**, *95*, 1–17.
93. Cantini, P.; Testa, G.; Zanchetta, G.; Cavallini, R. The Plio-Pleistocenic evolution of extensional tectonics in northern Tuscany, as constrained by new gravimetric data from the Montecarlo Basin (lower Arno Valley, Italy). *Tectonophysics* **2001**, *330*, 25–43. [CrossRef]
94. Puccinelli, A.; D'Amato Avanzi, G.; Perilli, N.; Verani, M. Note Illustrative Della Carta Geologica d'Italia, Scala 1:50.000, CARG Foglio 262 Pistoia, ISPRA, A.T.I.-S.El.CA.srl-L.A.C.srl-System Cart srl. 2015; p. 157. Available online: https://www.isprambiente.gov.it/Media/carg/262_PISTOIA/Foglio.html (accessed on 15 March 2021).
95. Zanchetta, G. Nuove osservazioni sui depositi esposti sul fianco sud-orientale delle colline delle Cerbaie (Valdarno Inferiore, Toscana). *IL Quat.* **1995**, *8*, 291–304.

96. Sarti, G.; Testa, G.; Zanchetta, G. A new stratigraphic insight of the Upper Pliocene-Lower Pleistocene succession of Lower Valdarno (Tuscany, Italy). *Geoacta* **2008**, *7*, 27–41.
97. Aguzzi, M.; Amorosi, A.; Sarti, G. Stratigraphic architecture of late quaternary deposits in the lower Arno plain (Tuscany, Italy). *Geol. Romana* **2005**, *38*, 1–10.
98. Aguzzi, M.; Amorosi, A.; Castorina, F.; Ricci Lucchi, M.; Sarti, G.; Vaiani, S.C. Stratigraphic architecture and aquifer systems in the eastern Valdarno Basin, Tuscany. *Geoacta* **2006**, *5*, 39–60.
99. Sbrana, A.; Marianelli, P.; Pasquini, G.; Costantini, P.; Palmieri, F.; Ciani, V.; Sbrana, M. The integration of 3D modeling and simulation to determine the energy potential of low-temperature geothermal systems in the Pisa (Italy) sedimentary plain. *Energies* **2018**, *11*, 1591. [CrossRef]
100. Pascucci, V. Neogene evolution of the Viareggio Basin, Northern Tuscany (Italy). *Geoacta* **2005**, *4*, 123–128.
101. Pascucci, V.; Martini, I.P.; Sagri, M.; Sandrelli, F. Effects of transverse structural lineaments on the Neogene-Quaternary basins of Tuscany (inner Northern Apennines, Italy). *Sediment. Process. Environ. Basins Tribut. Peter Friend* **2007**, *38*, 155–182.
102. Bigot, A. Aléa sismique de la regione de Pise (Italie): Etude morphostructural des failles bordières du Bassin de Viareggio. *Master Geosci. Montp.* **2010**, *28*, 108–112.
103. Giampietro, T. Architettura Strutturale e Zone di Danneggiamento in Zone di Trasferimento in Sistemi di Faglie Normali: Il Caso di Studio di Vecchiano (PI) e Modellizzazione Sperimentale. Diploma Thesis, Università di Pisa, Pisa, Italy, 2018; p. 195.
104. Porta, L. Kinematics of Faulting in Extensional Systems: Analogue Modelling and a Comparison with the Viareggio Basin Case Study. Diploma Thesis, Università di Pisa, Pisa, Italy, 2019; p. 144.
105. D'Amato Avanzi, G.; Nardi, I. Indizi di neotettonica nei Monti d'Oltre Serchio: Faglie distensive recenti al bordo della Pianura Pisana e depositi ciottolosi a quota 170 metri. *Boll. Soc. Geol. Ital.* **1993**, *112*, 601–604.
106. Federici, P.R. La tettonica recente dell'Appennino. I. Il bacino villafranchiano di Sarzana ed il suo significato nel quadro dei movimenti distensivi a NW delle Apuane. *Boll. Soc. Geol. Ital.* **1973**, *92*, 287–301.
107. Abbate, E.; Fanucci, F.; Benvenuti, M.; Bruni, P.; Cipriani, N.; Falorni, P.; Fazzuoli, M.; Morelli, D.; Pandeli, E.; Papini, M.; et al. *Note Illustrative della Carta Geologica d'Italia, scala 1:50.000, CARG Foglio 248 La Spezia, ISPRA*; Regione: Liguria, Italy, 2005; p. 204.
108. Bertoldi, R. Lineamenti palino-stratigrafici di depositi continentali del Pliocene–Pleistocene inferiore iniziale dell'Italia nord-occidentale. *Boll. Della Soc. Paleontol. Ital.* **1997**, *36*, 63–73.
109. Raggi, D.; Raggi, G. La bassa Val di Magra ed il sottosuolo della Piana Lunense, da Capellini ai giorni nostri. *Mem. Accad. Lunigianese Sci.* **2016**, *86*, 139–178.
110. Storti, F. Tectonics of Punta Bianca promontory: Insights for the evolution of the Northern Apennines-Northern Tyrrhenian Sea basin. *Tectonics* **1995**, *14*, 832–847. [CrossRef]
111. Serpelloni, E.; Pintori, F.; Gualandi, A.; Scoccimarro, E.; Cavaliere, A.; Anderlini, L.; Belardinelli, M.E.; Todesco, M. Hydrologically-induced karst deformation: Insights from GPS measurements in the Adria-Eurasia plate boundary zone. *J. Geophys. Res. Solid Earth* **2018**, *85*, 457. [CrossRef]
112. Altamimi, Z.; Métivier, L.; Rebischung, P.; Rouby, H.; Collilieux, X. ITRF2014 plate motion model. *Geophys. J. Int.* **2017**, *209*, 1906–1912. [CrossRef]
113. Tape, C.; Musé, P.; Simons, M.; Dong, D.; Webb, F. Multiscale estimation of GPS velocity fields. *Geophys. J. Int.* **2009**, *179*, 945–971. [CrossRef]
114. Serpelloni, E.; Vannucci, G.; Anderlini, L.; Bennett, R.A. Kinematics, seismotectonics and seismic potential of the eastern sector of the European Alps from GPS and seismic deformation data. *Tectonophysics* **2016**, *688*, 157–181. [CrossRef]
115. Chiaraluce, L.; Barchi, M.R.; Carannante, S.; Collettini, C.; Mirabella, F.; Pauselli, C.; Valoroso, L. The role of rheology, crustal structures and lithology in the seismicity distribution of the northern Apennines. *Tectonophysics* **2017**, *694*, 280–291. [CrossRef]
116. Mantovani, E.; Viti, M.; Cenni, M.; Babbucci, D.; Tamburelli, C.; Baglione, M.; D'Intinosante, V. Seismotectonics and present seismic hazard in the Tuscany-Romagna-Marche-Umbria Apennines (Italy). *J. Geodyn.* **2015**, *89*, 1–14. [CrossRef]
117. Basili, R.; Valensise, G.; Vannoli, P.; Burrato, P.; Fracassi, U.; Mariano, S.; Tiberti, M.; Boschi, E. The Database of Individual Seismogenic Sources (DISS), version 3: Summarizing 20 years of research on Italy's earthquakes geology. *Tectonophysics* **2008**, *453*, 20–43. [CrossRef]
118. Ferretti, G.; Massa, M.; Solarino, S. An improved method for recognition of seismic families: Application to the Garfagnana-Lunigiana Area, Italy. *Bull. Seismol. Soc. Am.* **2005**, *96*, 1903–1915. [CrossRef]
119. Stramondo, S.; Vannoli, P.; Cannelli, V.; Polcari, M.; Melini, D.; Samsonov, S.; Moro, M.; Bignami, C.; Saroli, M. X- and C-Band SAR Surface Displacement for the 2013 Lunigiana Earthquake (Northern Italy): A Breached Relay Ramp? *Ieee J. Sel. Top. Appl. Earth Obs. Remote Sens.* **2014**, *7*, 2746–2753. [CrossRef]
120. Pezzo, G.; Boncori, J.P.M.; Atzori, S.; Piccinini, D.; Antonioli, A.; Salvi, S. The 2013 Lunigiana (Central Italy) earthquake: Seismic source analysis from DInSAR and seismological data, and geodynamical implications for the northern Apennines. *Tectonophys* **2014**, *636*, 315–324. [CrossRef]
121. Tertulliani, A.; Maramai, A. Macroseismic evidence and site effects for the Lunigiana (Italy) 1995 Earthquake. *J. Seism.* **1998**, *2*, 209–222. [CrossRef]
122. Dominguez, S.; Avouac, J.-P.; Michel, R. Horizontal coseismic deformation of the 1999 Chi-Chi earthquake measured from SPOT satellite images: Implications for the seismic cycle along the western foothills of central Taiwan. *J. Geophys. Res. Space Phys.* **2003**, 108. [CrossRef]

123. Manighetti, I.; Tapponnier, P.; Gillot, P.Y.; Jacques, E.; Courtillot, V.; Armijo, R.; Ruegg, J.C.; King, G. Propagation of rifting along the Arabia-Somalia Plate Boundary: Into Afar. *J. Geophys. Res. Space Phys.* **1998**, *103*, 4947–4974. [CrossRef]
124. Westway, R.; Gawthorpe, R.; Tozzi, M. Seismological and field observations of the 1984 Lazio-Abruzzo earthquakes: Implications for the active tectonics of Italy. *Geophys. J.* **1989**, *98*, 489–514. [CrossRef]
125. Manighetti, I.; King, G.C.P.; Gaudemer, Y.; Scholz, C.H.; Doubre, C. Slip accumulation and lateral propagation of active normal faults in Afar. *J. Geophys. Res. Solid Earth* **2001**, *106*, 13667–13696. [CrossRef]
126. Tondi, E.; Jablonská, D.; Volatili, T.; Michele, M.; Mazzoli, S.; Pierantoni, P.P. The Campotosto linkage fault zone between the 2009 and 2016 seismic sequences of central Italy: Implications for seismic hazard analysis. *GSA Bull.* **2020**. [CrossRef]
127. Molli, G.; Meccheri, M. Structural inheritance and style of reactivation at mid-crustal levels: A case study from the Alpi Apuane (Tuscany, Italy). *Tectonophysics* **2012**, *579*, 74–87. [CrossRef]
128. Piazza, A.; Artoni, A.; Ogata, K. The Epiligurian wedge-top succession in the Enza Valley (northern Apennines): Evidence of a syn-depositional transpressive system. *Swiss J. Geosci.* **2016**, *109*, 17–36. [CrossRef]
129. Cuffaro, M.; Riguzzi, F.; Scrocca, D.; Antonioli, F.; Carminati, E.; Livani, M.; Doglioni, C. On the geodynamics of the northern Adriatic plate. *Rend. Lincei* **2010**, *21*, 253–279. [CrossRef]
130. Liotta, D.; Brogi, A. Plio-Quaternary fault kinematics in the Larderello geothermal area (Italy): Insights for the interpretation of the present stress field. *Geothermics* **2020**, *83*, 101714. [CrossRef]
131. Boncio, P.; Brozzetti, F.; Lavecchia, G. Architecture and seismotectonics of a regional low-angle normal fault zone in Central Italy. *Tectonics* **2000**, *19*, 1038–1055. [CrossRef]
132. Eva, E.; Solarino, S.; Boncio, P. HypoDD relocated seismicity in northern Apennines (Italy) preceding the 2013 seismic unrest: Seismotectonic implications for the Lunigiana-Garfagnana area. *Boll. Geofis. Teor. Appl.* **2014**, *55*, 739–754.
133. Galadini, F.; Falcucci, E.; Galli, P.; Giacco, B.; Gori, S.; Messina, P.; Moro, M.; Saroli, M.; Scardia, G.; Sposato, A. Time intervals to assess active and capable faults for engineering practices in Italy. *Eng. Geol.* **2012**, *139*, 50–65. [CrossRef]
134. Piccardi, L.; Vittori, E.; Blumetti, A.M.; Comerci, V.; Di Manna, P.; Guerrieri, L.; Baglione, M.; D'Intinosante, V. Mapping capable faulting hazard in a moderate-seismicity, high heat-flow environment: The Tuscia province (southern Tuscany-northern Latium, Italy). *Quat. Int.* **2017**, *451*, 11–36. [CrossRef]
135. Tinti, S.; Maramai, A.; Graziani, L. A new version of the European tsunami catalogue: Updating and revision. *Nat. Hazards Earth Syst. Sci.* **2001**, *1*, 255–262. [CrossRef]